Supplementary Material

Combustion of *n*-C_3–C_6 linear alcohols: an experimental and kinetic modeling study. Part II: speciation measurement in a jet-stirred reactor, ignition delay time measurement in a rapid compression machine, model validation and kinetic analysis.

M. Pelucchi[1*], S. Namysl[2], E. Ranzi[1], A. Rodriguez[2], C. Rizzo[1], K. P. Somers[3], Y. Zhang[4], O. Herbinet[2], H.J. Curran[3], F. Battin-Leclerc[2], T. Faravelli[1].

[1] *CRECK Modeling Lab, Department of Chemistry Materials and Chemical Engineering, Politecnico di Milano, 20133, Milano, Italy*

[2] *Laboratoire Réactions et Génie des Procédés, CNRS, Université de Lorraine, ENSIC, Nancy Cedex, France*

[3] *Combustion Chemistry Centre, National University of Ireland Galway, Galway, Ireland*

[4] *State Key Laboratory of Multiphase Flow in Power Engineering, Xi'an Jiaotong University, Xi'an 710049, China*

Corresponding author:

Dr. Matteo Pelucchi,

Department of Chemistry, Materials

and Chemical Engineering,

Politecnico di Milano, Milan, Italy

Email: matteo.pelucchi@polimi.it

Tel: +39 02 2399 4234

Contents:

1. Mixture compositions for RCM experiments

Table S1. Alcohol/air mixtures (% mole fraction) tested in this study.

Mix No.	Fuel Type	X_{Fuel}	X_{O2}	X_{N2}	X_{Ar}	X_{CO2}	Temperature/K	ϕ	P [atm]
1	Ethanol	6.53	19.63	36.92	36.92	0.00	893-926	1.0	10
2		6.53	19.63	29.53	44.31	0.00	826-909	1.0	30
3	*n*-propanol	4.46	20.08	37.73	37.73	0.00	800-935	1.0	10 and 30
4	*n*-butanol	3.38	20.29	22.90	53.43	0.00	724-824	1.0	10
5		3.38	20.29	68.70	7.63	0.00	727-844	1.0	30
6		3.38	20.29	53.43	0.00	22.90	704-735	1.0	30
7	*n*-pentanol	2.72	20.43	76.85	0.00	0.00	710-833	1.0	10
8		2.72	20.43	38.42	38.43	0.00	813-926	1.0	10

2. Experimental ignition delay times

Table S2 shows measured ignition delay times. Volume profiles obtained from pressure traces of non reactive experiments are reported in Excel format in the Supplementary Material. To reduce the data points, and improve the speed of RCM simulations, for each non-reactive volume trace the Segment Fit approach was used. The impact of non-reactive pressure-time history made of data points from 10 to 100, in multiples of 10, was tested. Only negligible differences in the compression peak pressure observed which do not affect the IDT simulation, were observed, especially taking the points from 20 onwards.

Table S2. Experimental ignition delay time data in RCM.

Ethanol

P=10 atm, ϕ = 1.0			P=30 atm, ϕ = 1.0		
P_c [atm]	T_c [K]	IDT [ms]	P_c [atm]	T_c [K]	IDT [ms]
10.14	889	134.1	29.66	828	118.9
10.19	890	134.4	29.51	827	142.1
10.14	889	135.9	29.32	826	141.1
10.14	908	48.6	29.95	847	45.4
10.14	908	48.4	29.87	846	44.4
10.25	910	50.2	29.96	847	49.1
10.17	929	17.6	29.94	868	19.8
10.20	930	17.2	29.83	867	19.3
10.20	930	17.6	29.96	868	20.4
			29.97	889	10.1

	30.05	890	10.5
	29.98	889	10.3
	29.76	888	10.2
	30.01	913	5.54
	30.23	912	5.21
	30.12	911	5.39

n-propanol

P=10 atm, ϕ = 1.0			P=30 atm, ϕ = 1.0		
P_c [atm]	T_c [K]	IDT [ms]	P_c [atm]	T_c [K]	IDT [ms]
10.26	875	136.4	30.29	803	133.5
10.26	875	126.3	30.26	803	156.3
10.22	875	119.1	30.30	803	124.9
10.16	874	120.5	30.36	804	149.1
10.22	895	46.5	29.45	815	89.9
10.17	894	44.9	30.38	817	86.5
10.23	896	40.4	30.07	817	89.3
10.24	916	20.8	29.86	815	79.5
10.26	916	19.2	29.71	814	85.2
10.21	916	19.5	30.45	840	34.8
10.05	935	11.9	29.74	836	32.0
10.12	936	10.6	30.03	838	29.6
10.16	937	9.48	30.26	838	35.8
			29.75	836	31.6
			30.12	860	15.9
			29.84	858	15.8
			29.99	860	15.0
			30.04	880	8.78
			30.01	879	9.12
			30.05	880	8.86
			29.91	900	4.75
			30.03	900	4.41
			30.01	900	4.41

n-butanol

P=10 atm, ϕ = 1.0			P=30 atm, ϕ = 1.0		
P_c [atm]	T_c [K]	IDT [ms]	P_c [atm]	T_c [K]	IDT [ms]
9.86	824	143.8	29.12	727	22.4
9.74	822	145.8	30.17	727	21.3
10.02	822	135.8	30.05	727	20.9
10.08	824	130.7	29.84	726	21.3
10.09	838	100.6	29.09	741	14.1
10.17	839	115.2	30.05	741	13.2
10.14	839	103.4	30.6	744	12.4
10.22	840	118.2	30.11	742	12.5
10.32	847	81.8	30.25	762	9.28
10.29	847	81.6	30.09	762	9.59
10.11	844	77.3	30.48	764	9.98
9.92	858	47.0	30.84	785	8.11
9.85	859	42.0	30.64	785	8.39
9.84	859	43.2	30.66	785	8.56
10.16	882	26.5	30.63	785	8.53
9.97	880	27.6	30.31	803	7.82
10.10	882	25.8	30.68	805	7.35
10.04	902	15.8	30.77	805	7.59
10.24	906	15.1	30.27	802	7.33
10.21	905	16.1	30.52	824	6.01
10.16	925	7.50	30.31	825	6.06
10.11	924	7.83	29.9	823	5.91
10.11	924	7.56	30.34	825	6.11
			30.26	845	5.08
			30.21	844	4.88
			30.19	844	5.04
			29.6	703	154.7
			30.16	704	111
			29.78	702	118.3
			30.29	704	100.6
			29.47	717	54.2
			30.65	720	55.7
			30.4	720	55
			29.64	734	28.8
			30.15	736	28
			30.09	736	26.1

n-pentanol

P=10 atm, ϕ = 1.0		
P_c [atm]	T_c [K]	IDT [ms]
10.65	711	85.0
10.59	710	77.7
10.05	711	76.3
10.03	710	77.2
9.79	725	45.4
10.02	725	47.5
10.02	725	44.1
9.96	743	26.9
10.04	744	30.3
9.90	742	28.9
9.95	743	27.1
9.98	761	25.9
9.99	762	24.1
10.03	762	23.1
9.92	779	26.2
10.05	781	24.5
10.01	780	23.9
9.95	797	27.6
9.93	796	26.6
9.99	797	27.0
10.08	817	30.5
10.07	816	31.3
10.18	818	31.1
10.26	837	32.0
10.15	836	31.6
10.24	838	33.3
9.943	845	32.9
10.14	849	28.5
10.13	848	29.4
10.02	869	28.0
10.03	869	29.1
9.99	869	26.5
10.10	890	24.8
10.11	890	22.2
9.99	888	24.1
10.23	912	13.6
10.19	912	13.9
10.08	908	13.9
10.10	929	9.64
10.17	931	9.44
10.15	930	9.04

3. Additional validation targets for *n*-C_3-C_6 alcohols pyrolysis and oxidation

Pyrolysis (Hefei Flow Reactor [1-3])

Figure S1 compares model results with pyrolysis speciation experiments at p=30, 200 and 760 Torr for *n*-propanol (3% mol) diluted in Argon (97% mol).

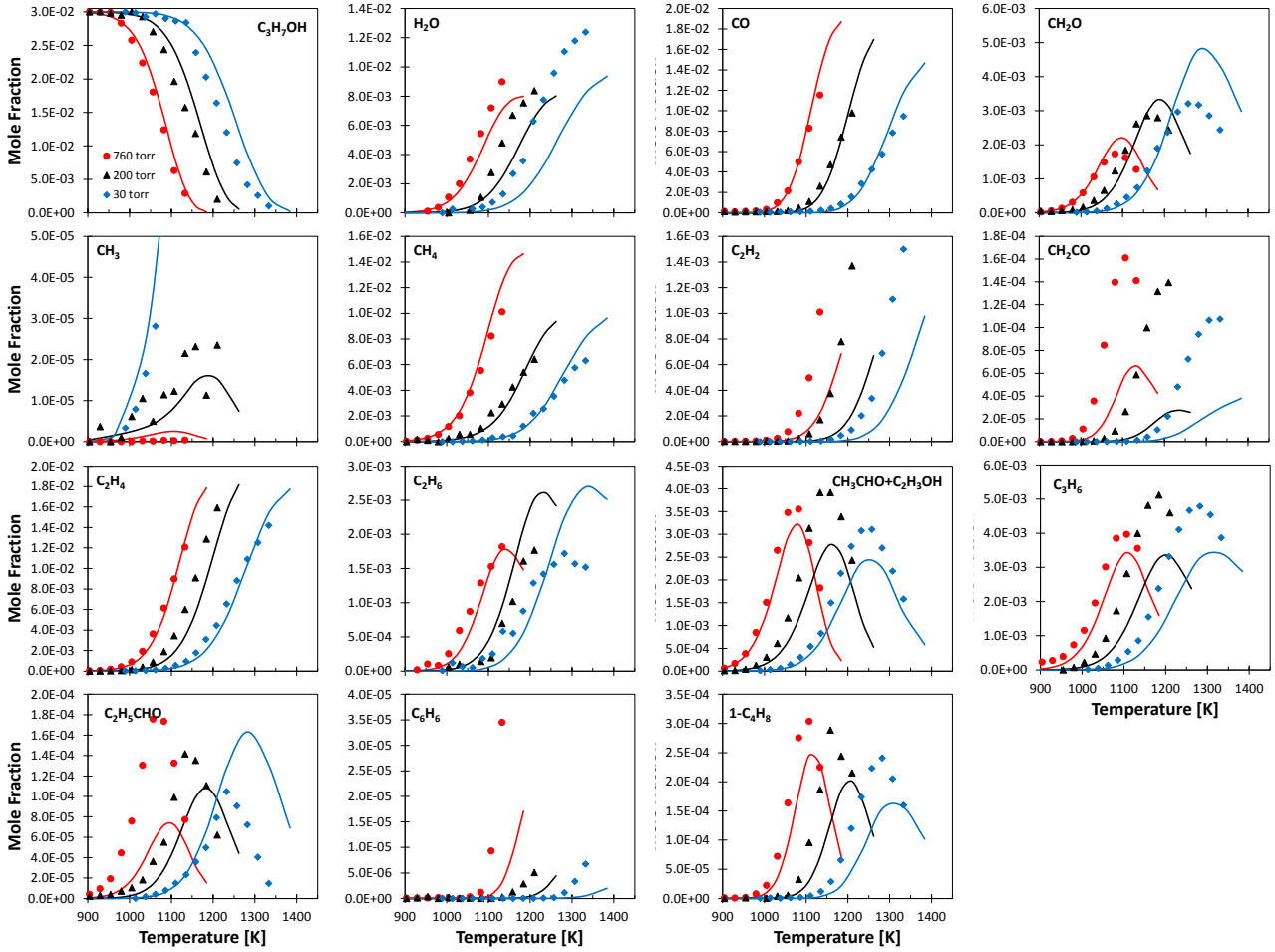

Figure S1: Experimental [1](symbols) and simulated (solid lines) mole fraction profiles of n-propanol pyrolysis at p = 30, 150 and 760 Torr. Composition: 3% fuel, 97% argon.

Figure S2 compares model results with pyrolysis speciation experiments at p=30, 200 and 760 Torr for *n*-butanol (3% mol) diluted in Argon (97% mol).

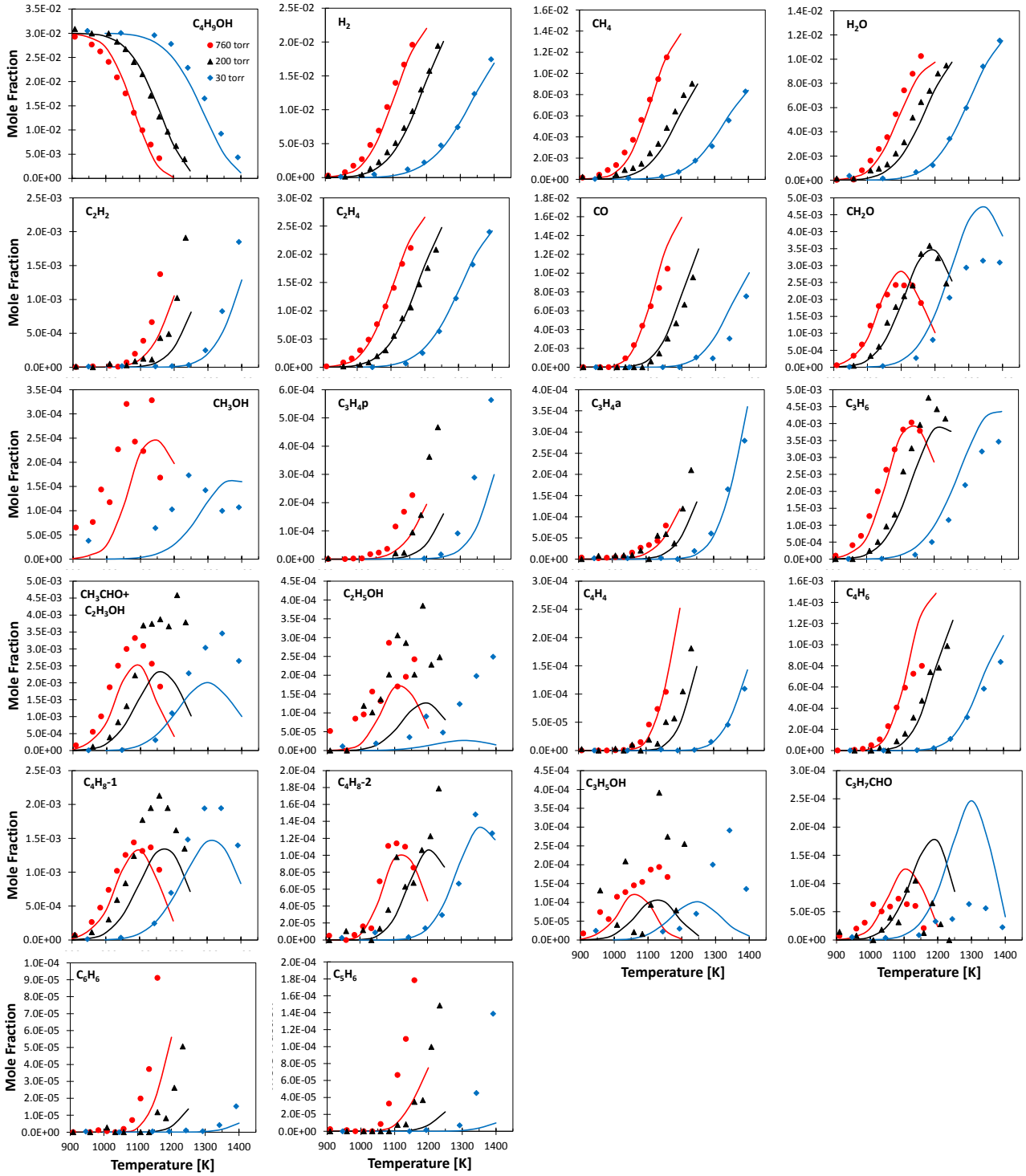

Figure S2: Experimental [2] (symbols) and simulated (solid lines) mole fraction profiles of n-butanol pyrolysis at p = 30, 200 and 760 Torr. Composition: 3% fuel, 97% argon.

Figure S3 compares model results with pyrolysis speciation experiments at p=30, 150 and 760 Torr for *n*-pentanol (3% mol) diluted in Argon (97% mol).

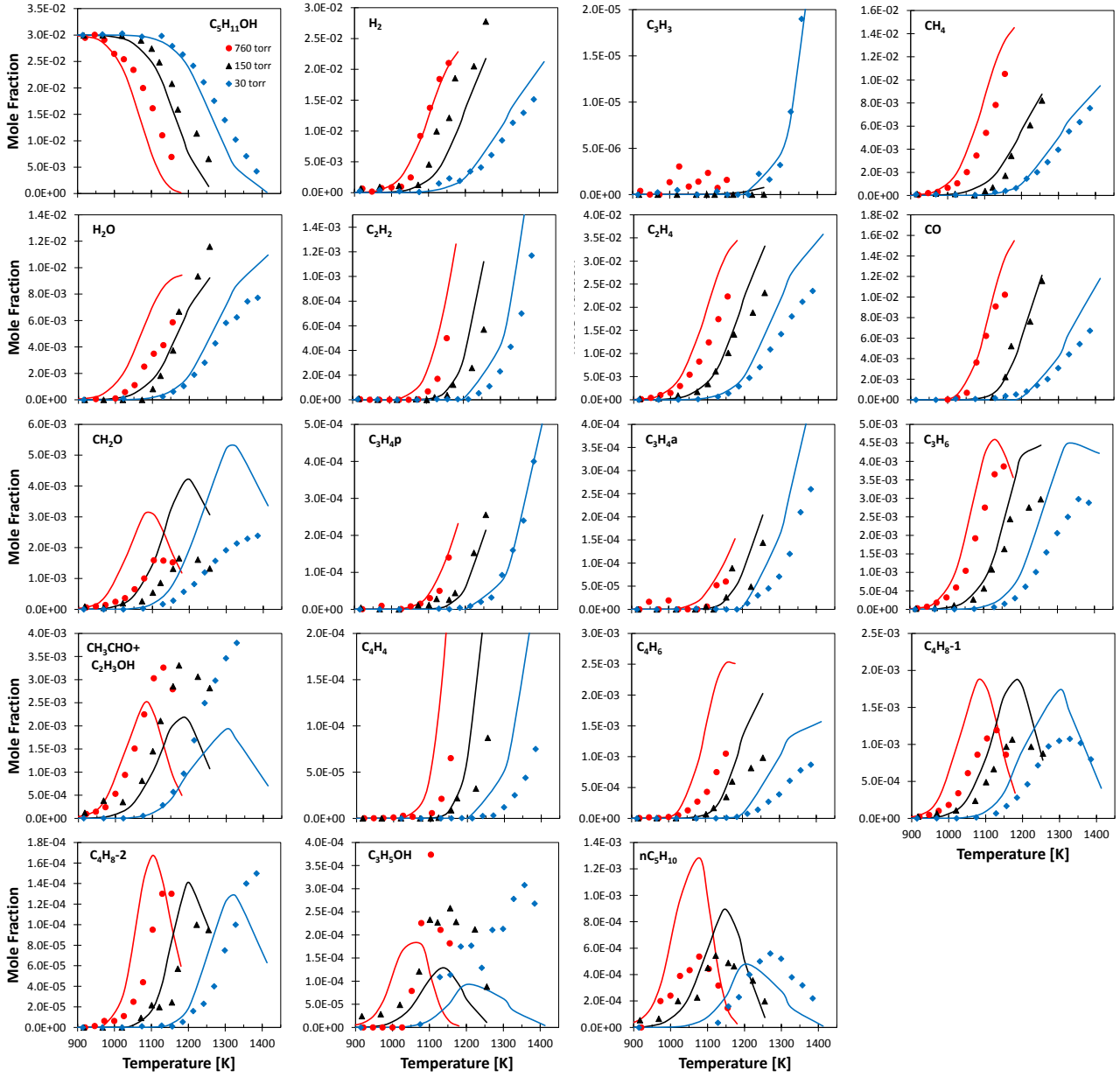

Figure S3: Experimental (symbols) and simulated (solid lines) mole fraction profiles of n-pentanol pyrolysis at p = 30, 150 and 760 Torr. Composition: 3% fuel, 97% argon.

Figure S4 compares results from the kinetic model presented in this work and those from the model of Sarathy et al. [4] with the experimental data for *n*-pentanol pyrolysis at p=760 Torr [3].

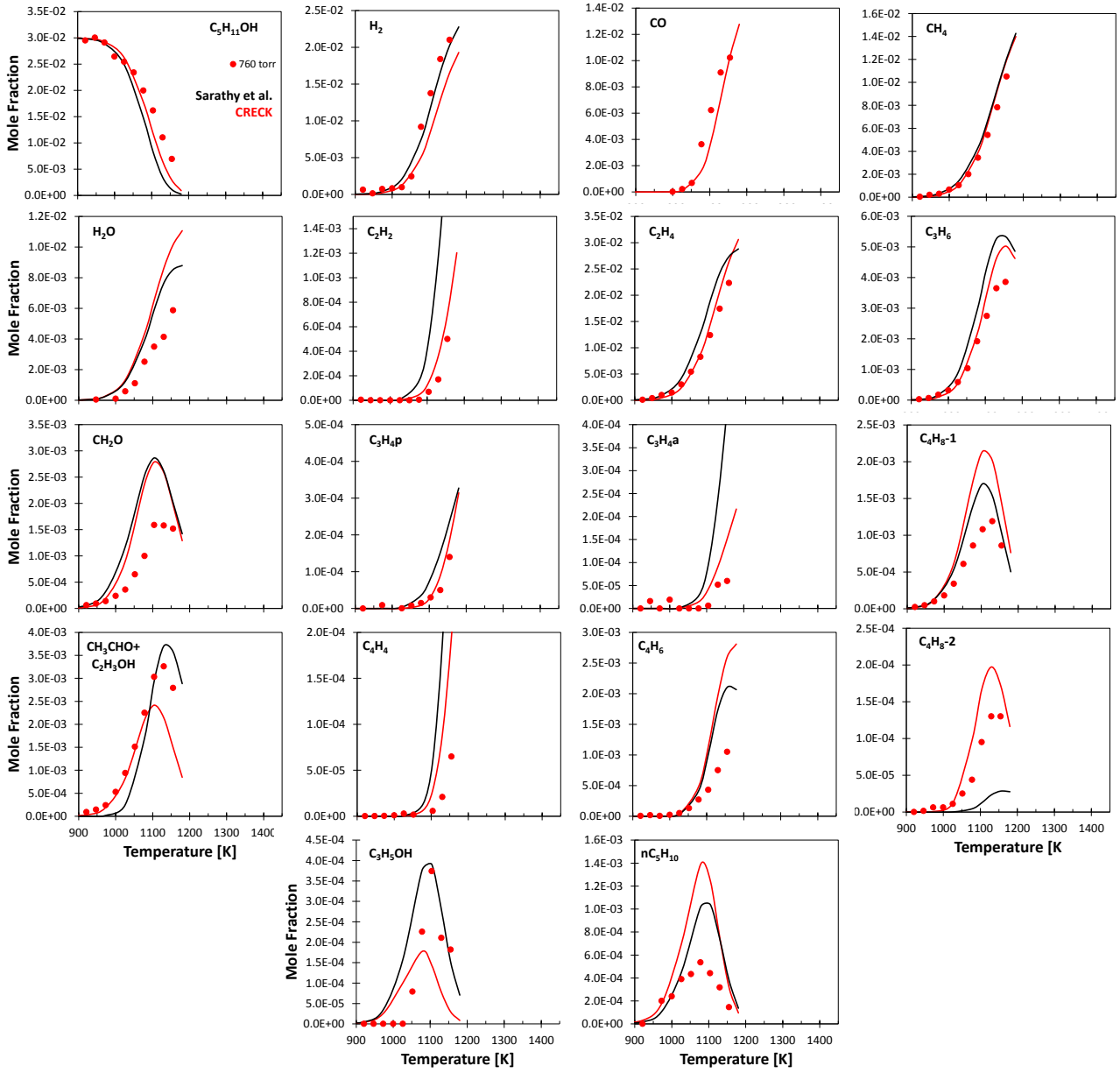

Figure S4: Experimental (symbols) and simulated (solid lines) mole fraction profiles of n-pentanol pyrolysis at p = 760 Torr. Composition: 3% fuel, 97% argon. Black lines: Sarathy et al. [4], red lines: this work.

Oxidation in Nancy JSR

Figure S5 and Figure S6 compare model results with oxidation speciation measurements carried out in this work in the jet-stirred reactor at CNRS Nancy. In addition to the ϕ=1.0 case reported in the manuscript we report results for the ϕ=0.5 and 2.0 cases in Figure S5 and Figure S6, respectively.

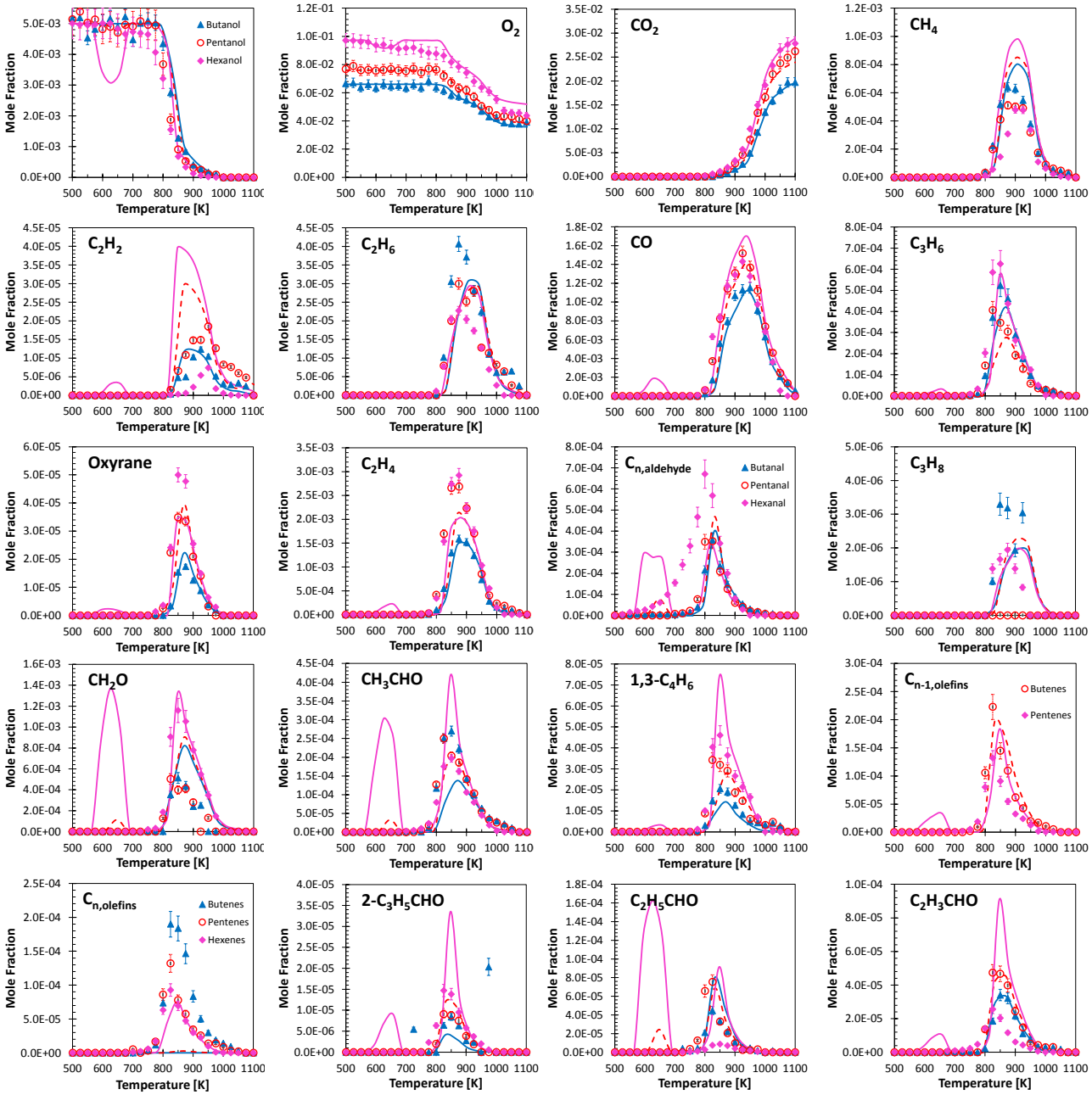

Figure S5: n-butanol, n-pentanol and n-hexanol oxidation in JSR at φ = 0.5, p = 107 kPa and τ = 2.0 s. Comparison between experimental (symbols) and predicted (lines) mole fraction profiles of intermediate and product species.

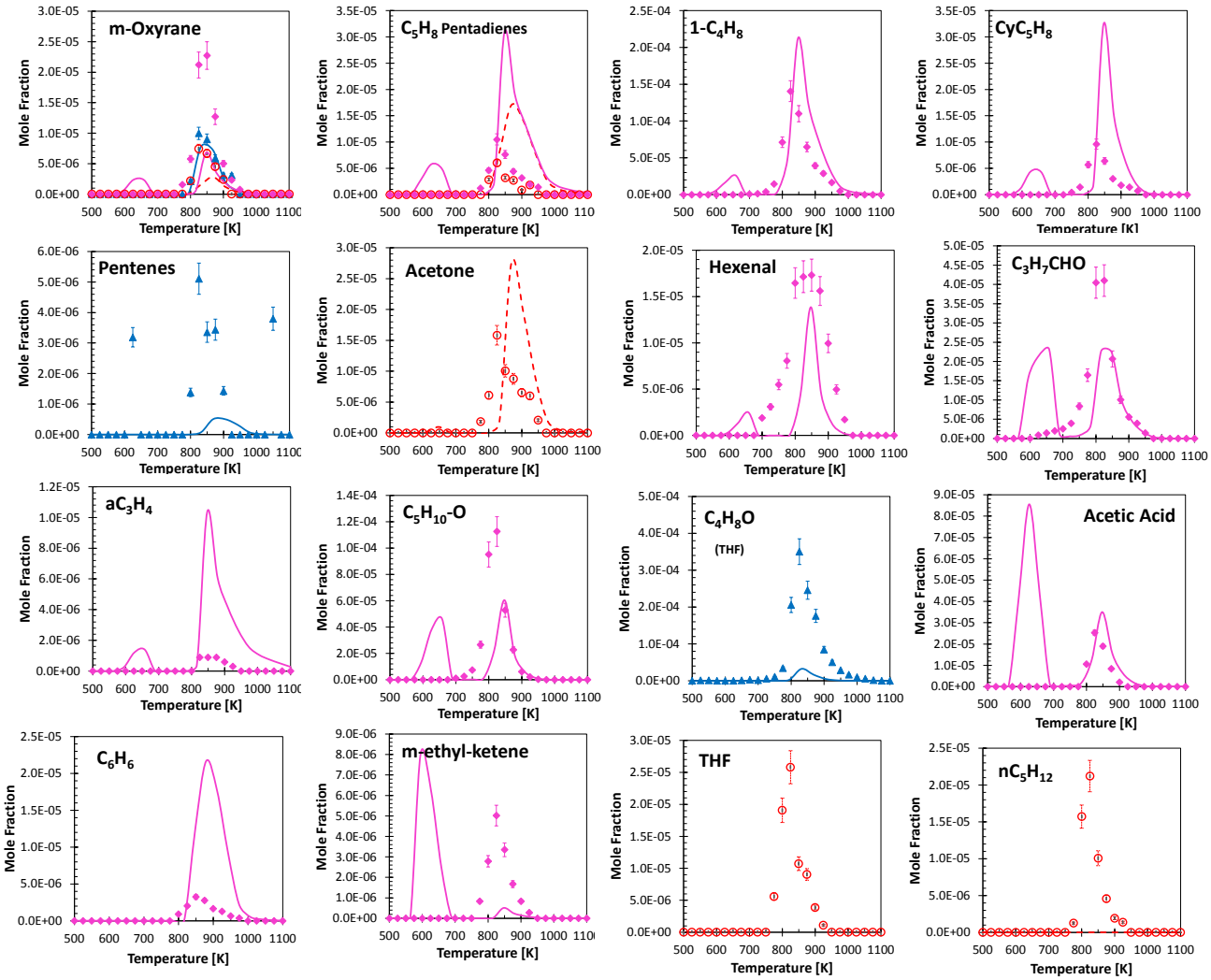

Figure S5: continued.

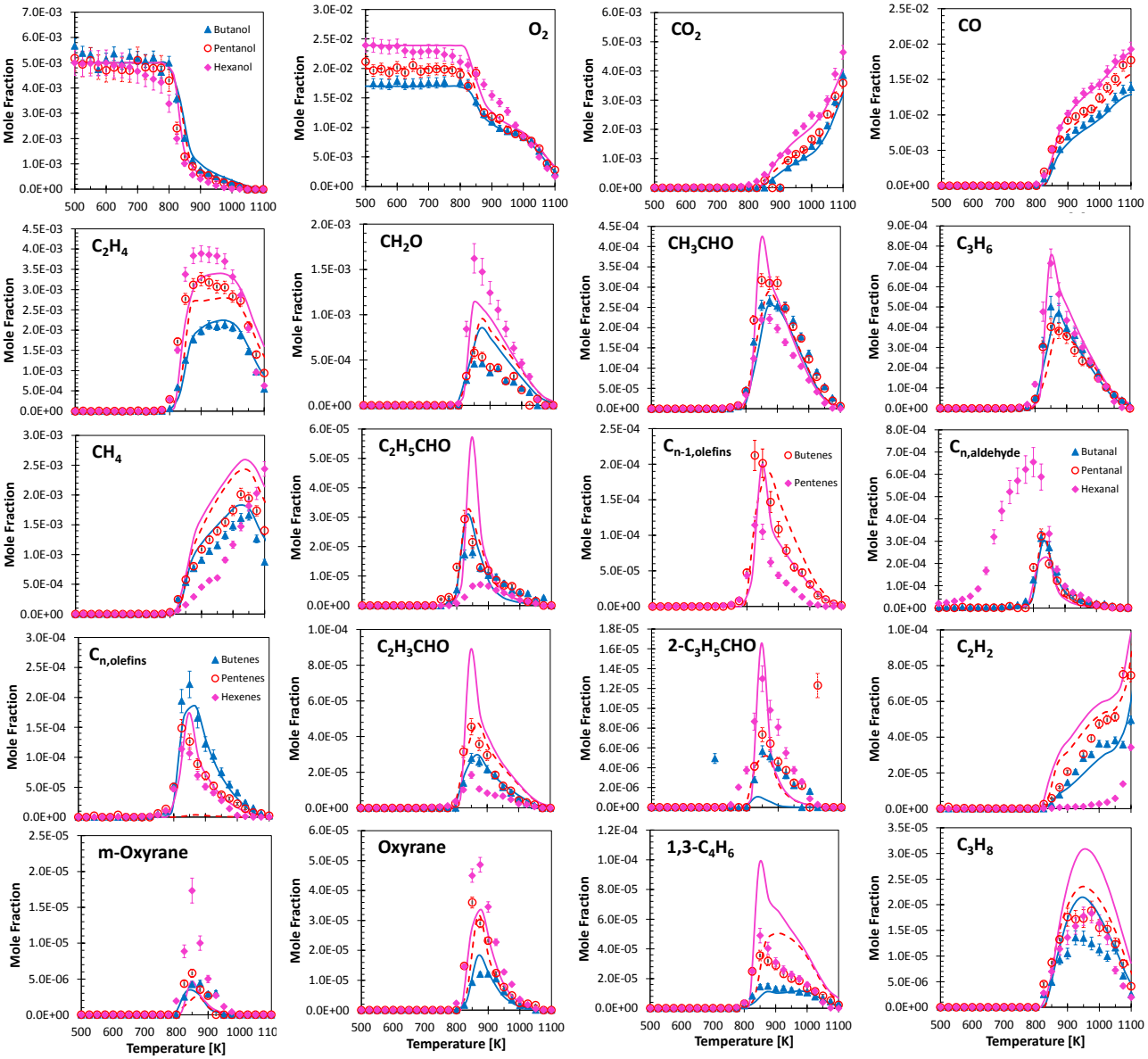

Figure S6: n-butanol, n-pentanol and n-hexanol (0.5 % mol) oxidation in JSR at φ = 2.0, p = 107 kPa and τ = 2.0 s. Comparison between experimental (symbols) and predicted (lines) mole fraction profiles of intermediate and product species.

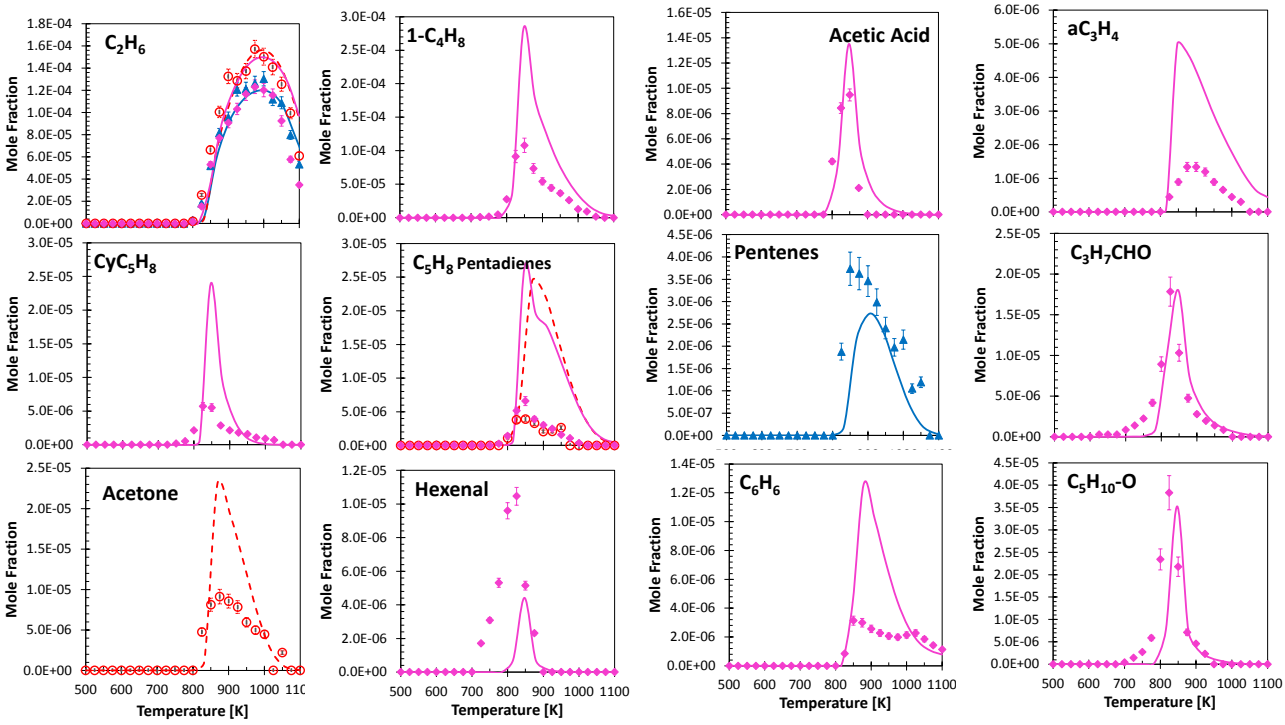

Figure S6: continued.

Figure S7 compares the model presented in this work with that of Sarathy et al. [4] for the oxidation of a stoichiometric *n*-pentanol (0.5 % mol)/O_2/N_2 mixture at p=107 kPa and τ=2.0 s (experimental measurement from this work).

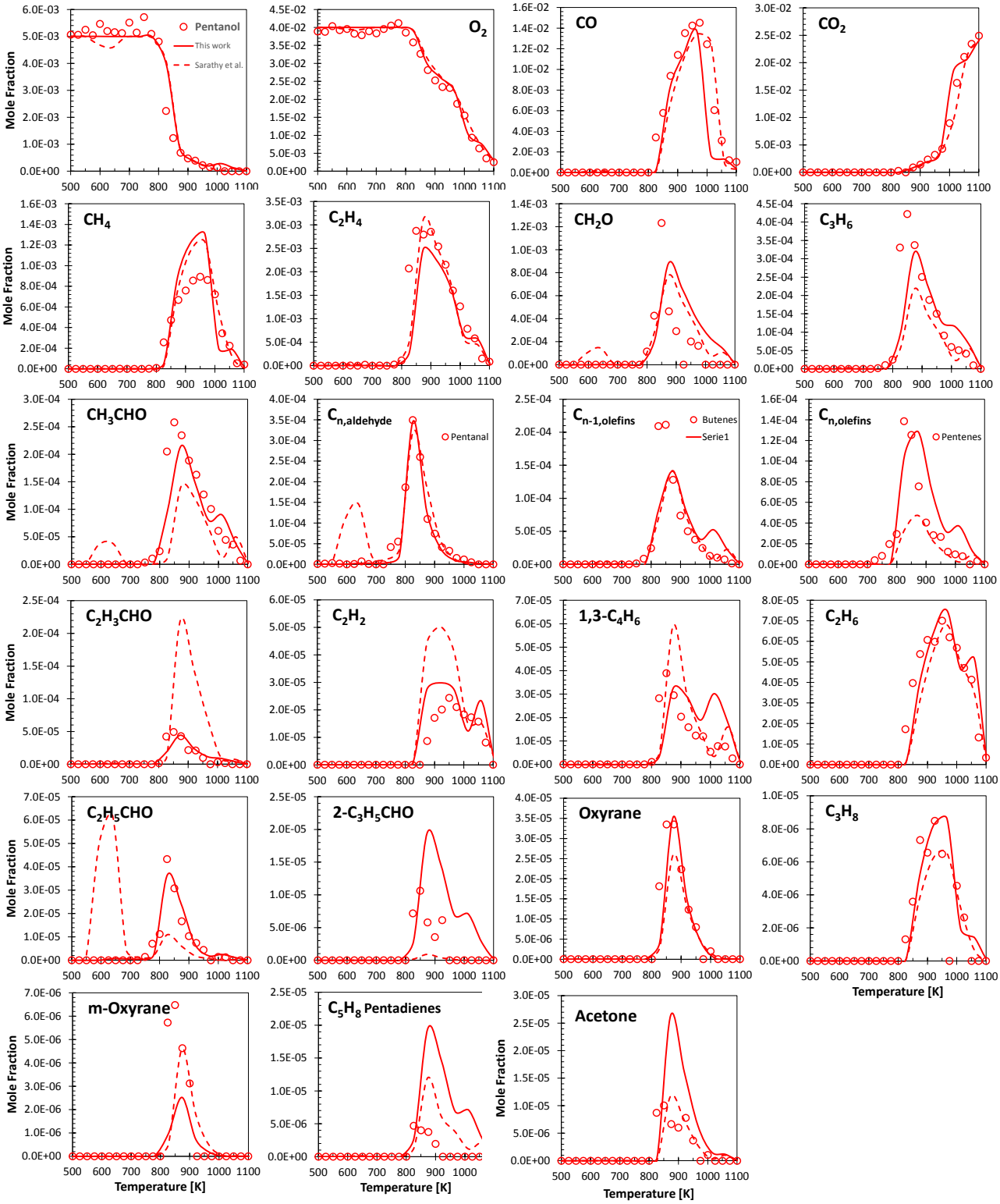

Figure S7: Experimental (symbols, this work) and simulated (lines) mole fraction profiles of n-pentanol oxidation at p = 107 kPa and φ=1.0. Dashed lines: Sarathy et al. [4], solid lines: this work.

Oxidation in Orléans JSR [5-9]

Figures S8, S9, S10 and S11 compare model results with oxidation speciation measurements [5] of *n*-propanol (0.15 % mol)/O_2/N_2 mixtures in Orléans jet-stirred reactor at p=10 bar, τ=0.7 s and ϕ=0.35, 0.5, 1.0 and 2.0.

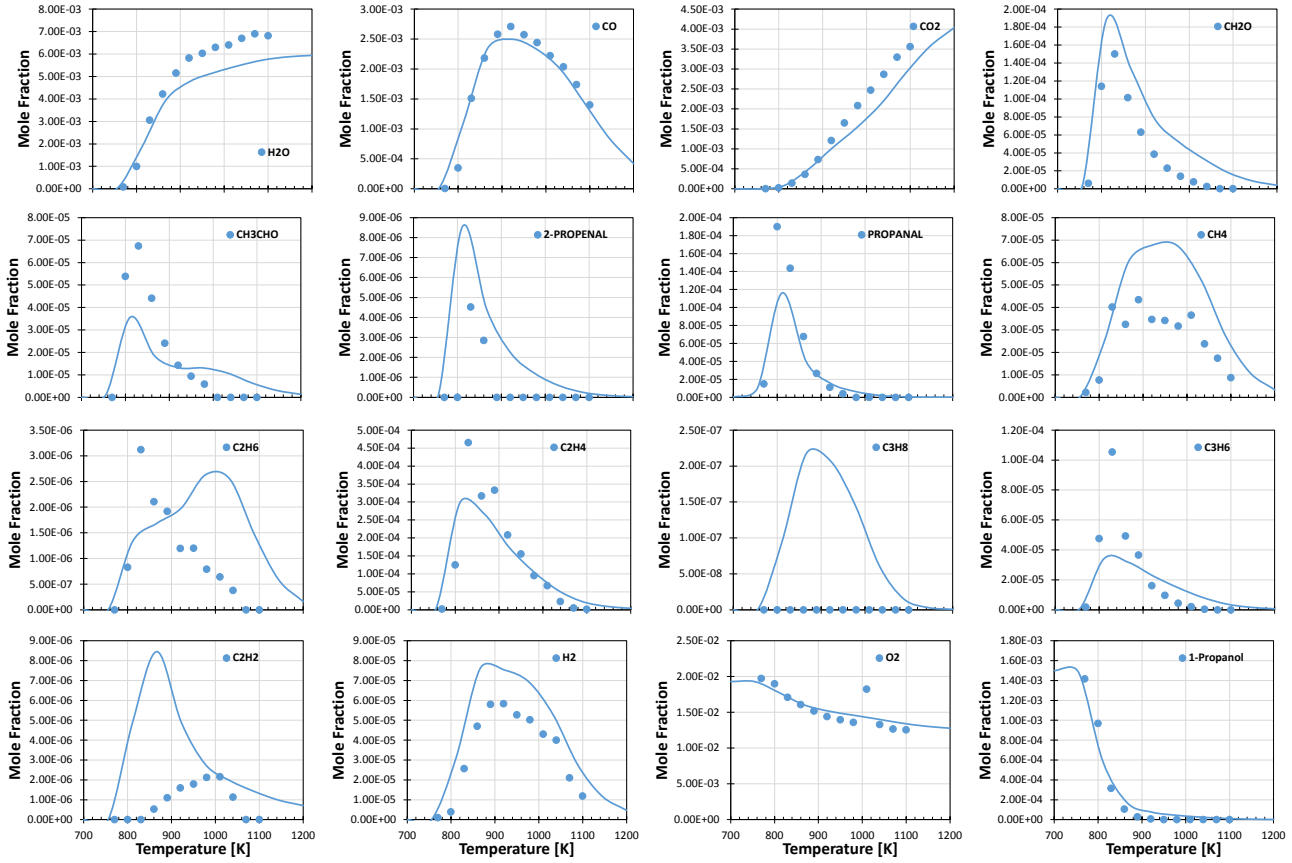

Figure S8: n-propanol (0.15% mol)/O_2/N_2 oxidation in JSR at φ = 0.35, p = 10 bar and τ = 0.7 s. Comparison between experimental (symbols) and predicted (lines) mole fraction profiles of intermediate and product species.

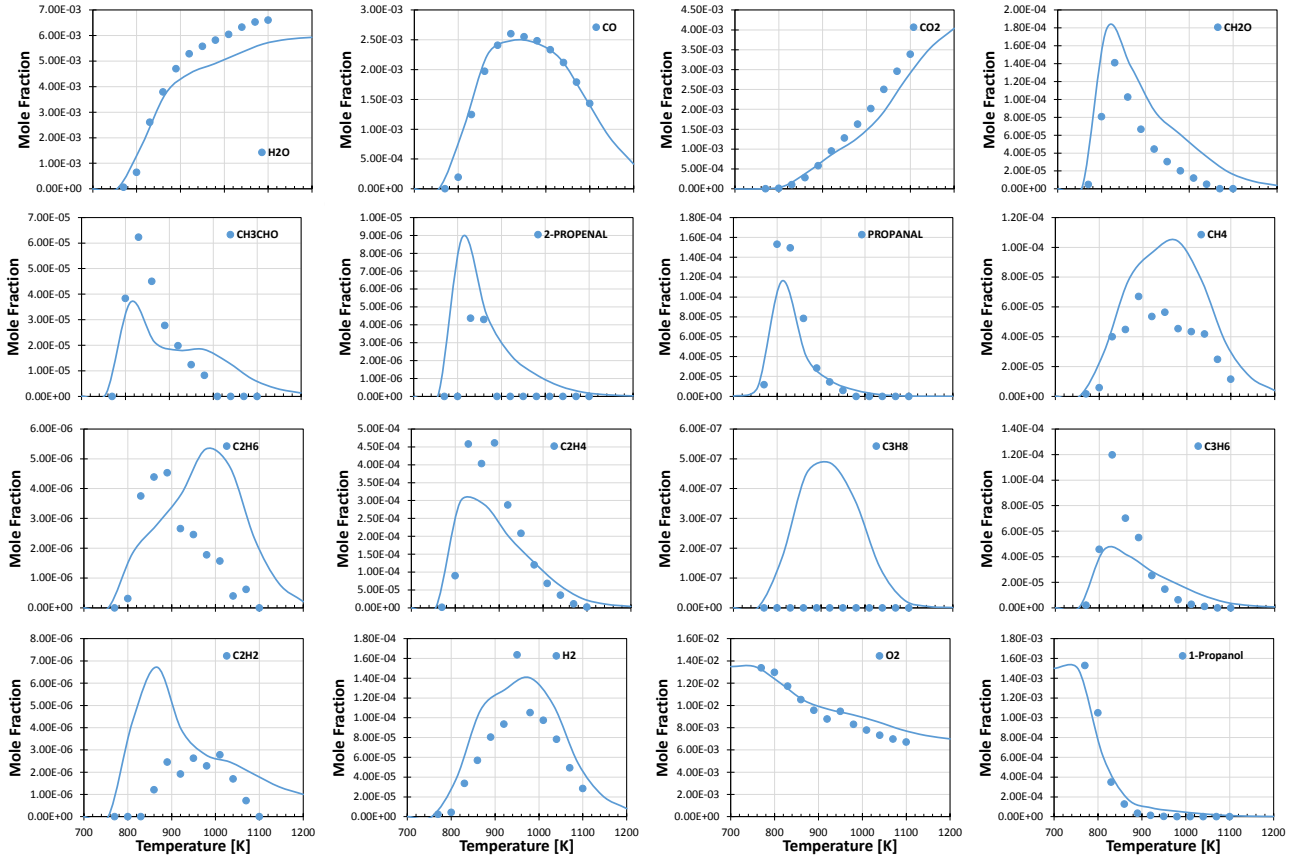

Figure S9: n-propanol (0.15% mol)/O_2/N_2 oxidation in JSR at φ = 0.5, p = 10 bar and τ = 0.7 s. Comparison between experimental (symbols) and predicted (lines) mole fraction profiles of intermediate and product species.

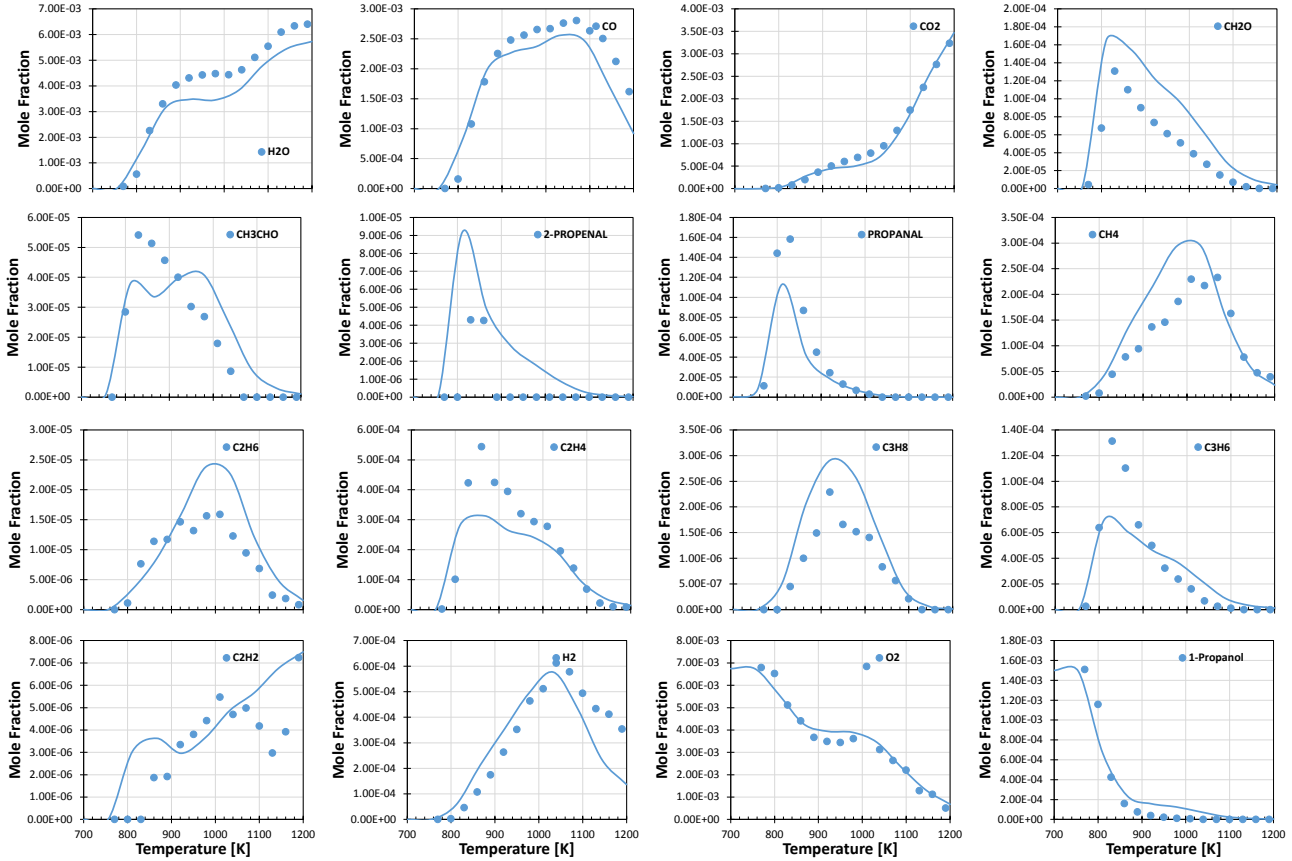

Figure S10: n-propanol (0.15% mol)/O_2/N_2 oxidation in JSR at φ = 1.0, p = 10 bar and τ = 0.7 s. Comparison between experimental (symbols) and predicted (lines) mole fraction profiles of intermediate and product species.

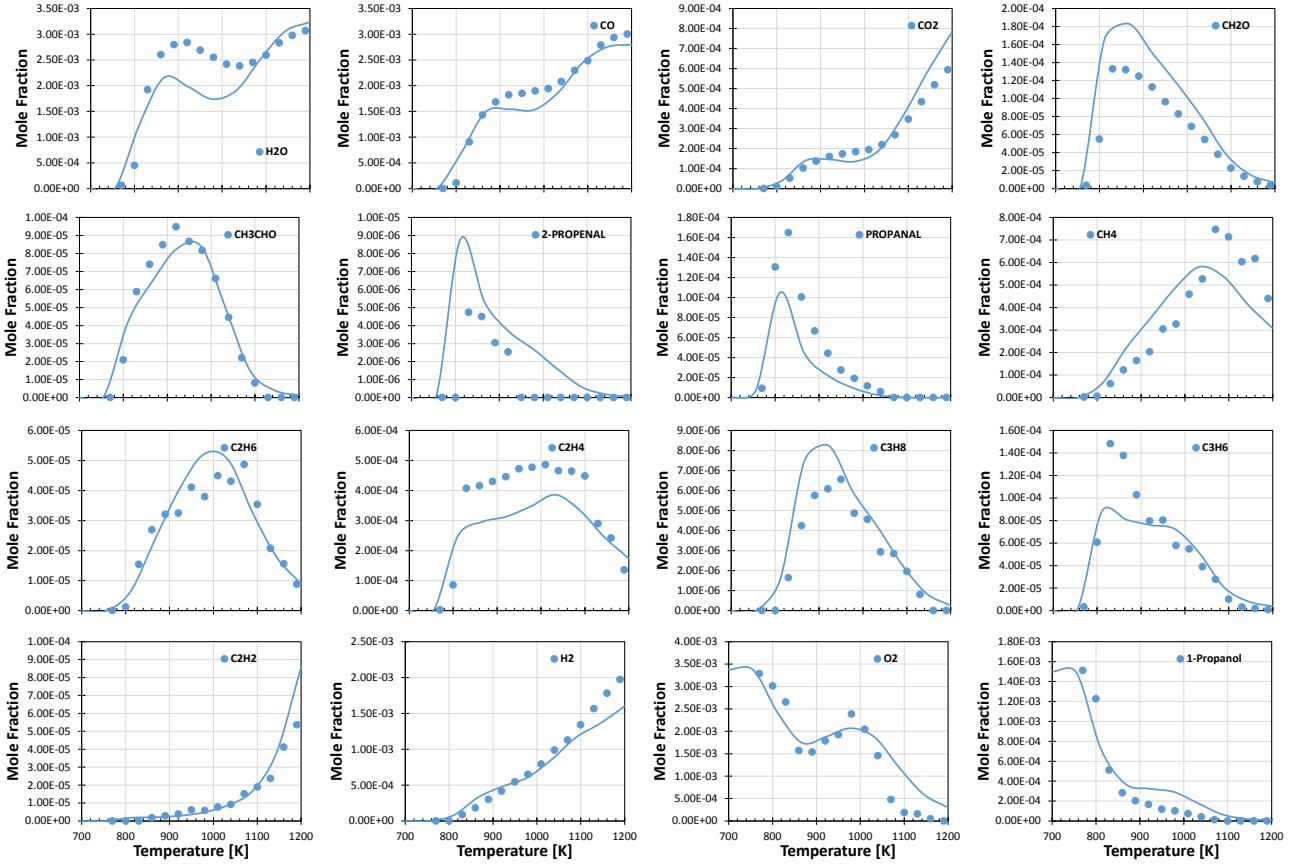

Figure S11: n-propanol (0.15% mol)/O_2/N_2 oxidation in JSR at φ = 2.0, p = 10 bar and τ = 0.7 s. Comparison between experimental (symbols) and predicted (lines) mole fraction profiles of intermediate and product species.

Figures S12 and S13 compare model results with oxidation speciation measurements [6, 8, 9] of *n*-butanol, *n*-pentanol, *n*-hexanol (0.1 % mol)/O_2/N_2 mixtures in Orléans jet-stirred reactor at p=10 bar, τ=0.7 s and ϕ=0.5 and 2.0, respectively.

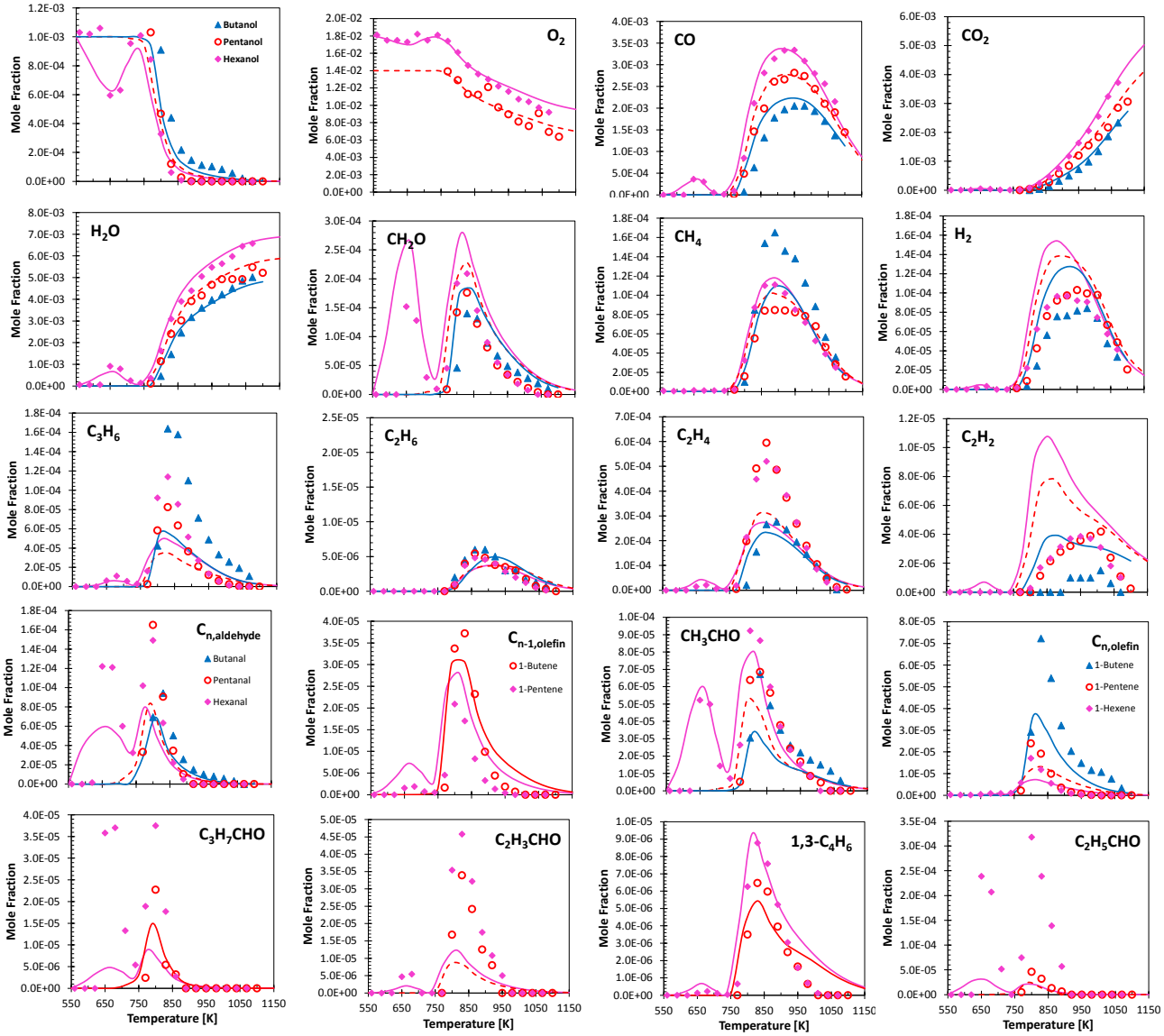

Figure S12: n-butanol, n-pentanol and n-hexanol (0.1 % mol)/O_2/N_2 mixtures oxidation in JSR at φ = 0.5, p = 10 bar and τ = 0.7 s. Comparison between experimental (symbols) [6, 8, 9] and predicted (lines) mole fraction profiles of intermediate and product species.

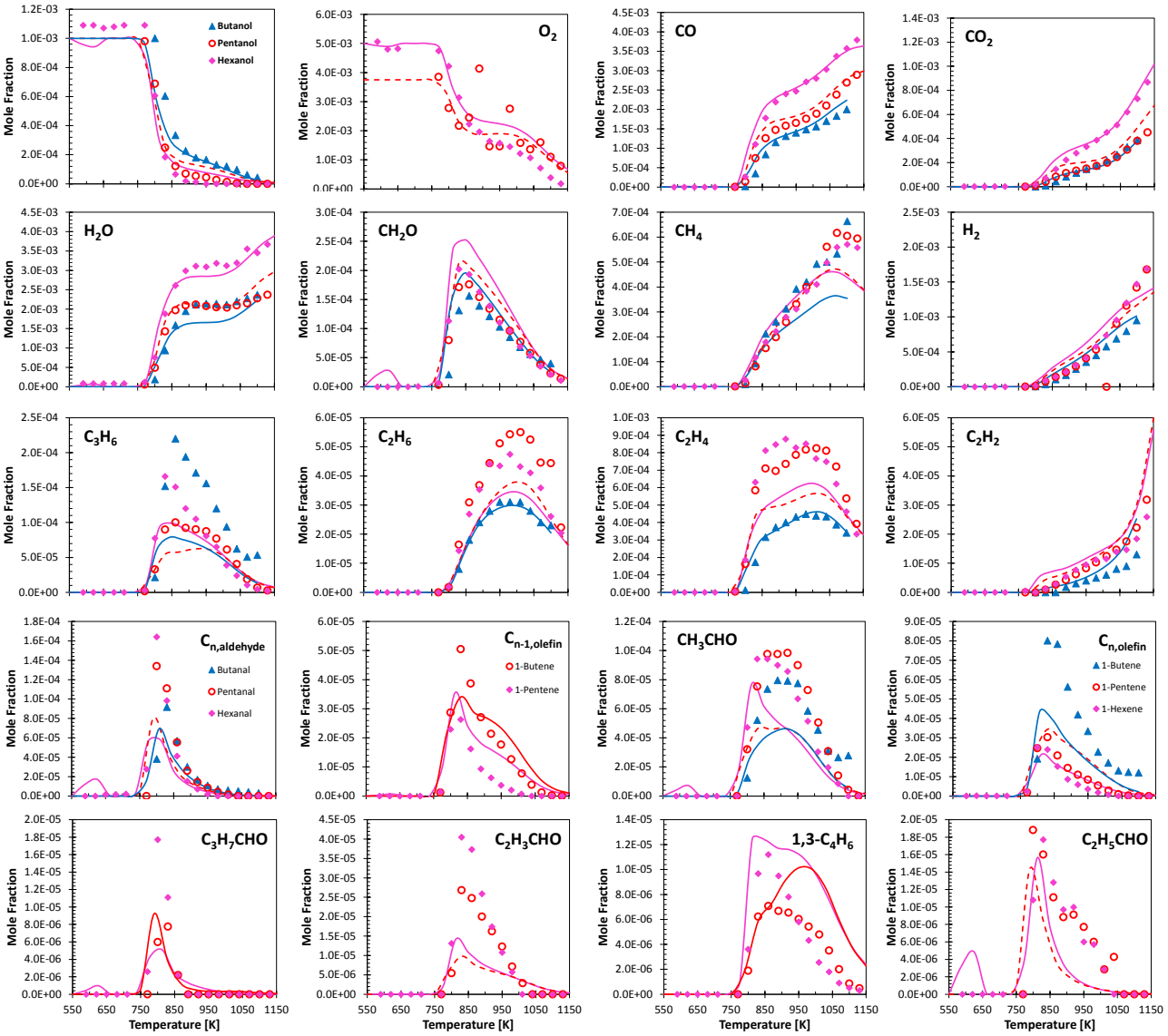

Figure S13: n-butanol, n-pentanol and n-hexanol (0.1 % mol)/O_2/N_2 mixtures oxidation in JSR at φ = 2.0, p = 10 bar and τ = 0.7 s. Comparison between experimental (symbols) [6, 8, 9] and predicted (lines) mole fraction profiles of intermediate and product species.

Figures S14, S15, S16 and S17 compare model results with speciation measurements of *n*-butanol (0.1 % mol)/O_2/N_2 mixtures in Orléans jet-stirred reactor at p=1 bar, τ=0.07 s and ϕ=0.25, 0.5, 1.0 and 2.0, respectively.

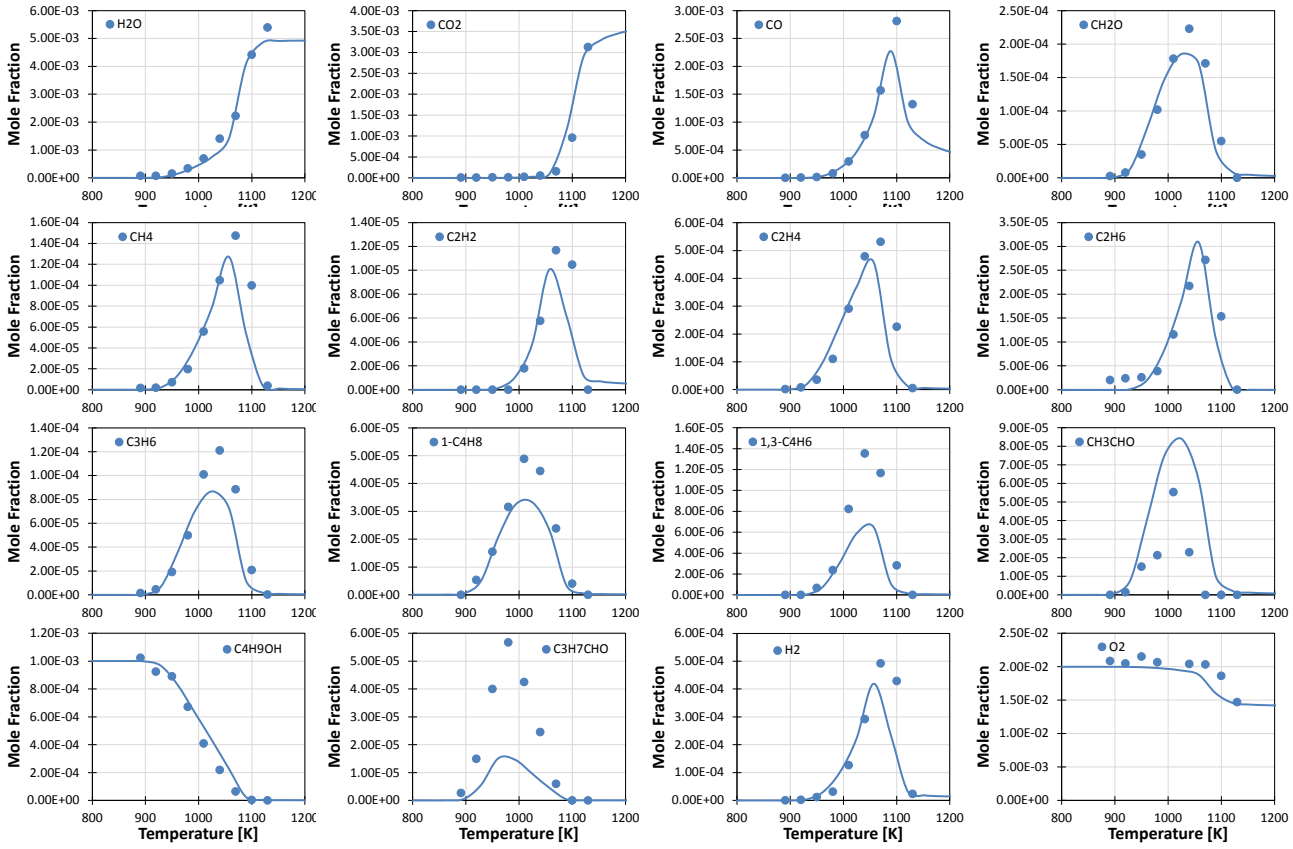

Figure S14: n-butanol (0.1% mol)/O_2/N_2 oxidation in JSR at φ = 0.25, p = 1 bar and τ = 0.07 s. Comparison between experimental (symbols) [7] and predicted (lines) mole fraction profiles of intermediate and product species.

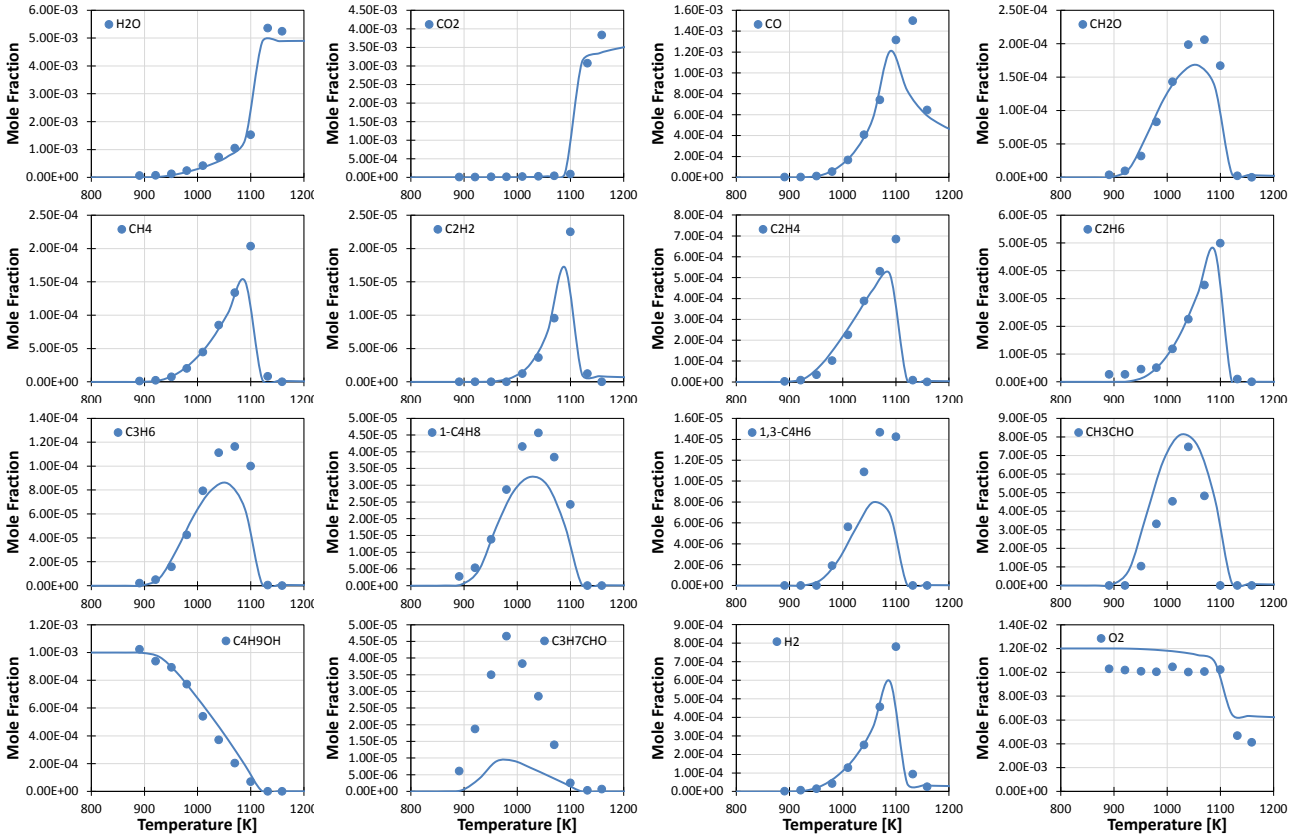

Figure S15: n-butanol (0.1% mol)/O_2/N_2 oxidation in JSR at φ = 0.5, p = 1 bar and τ = 0.07 s. Comparison between experimental (symbols) [7] and predicted (lines) mole fraction profiles of intermediate and product species.

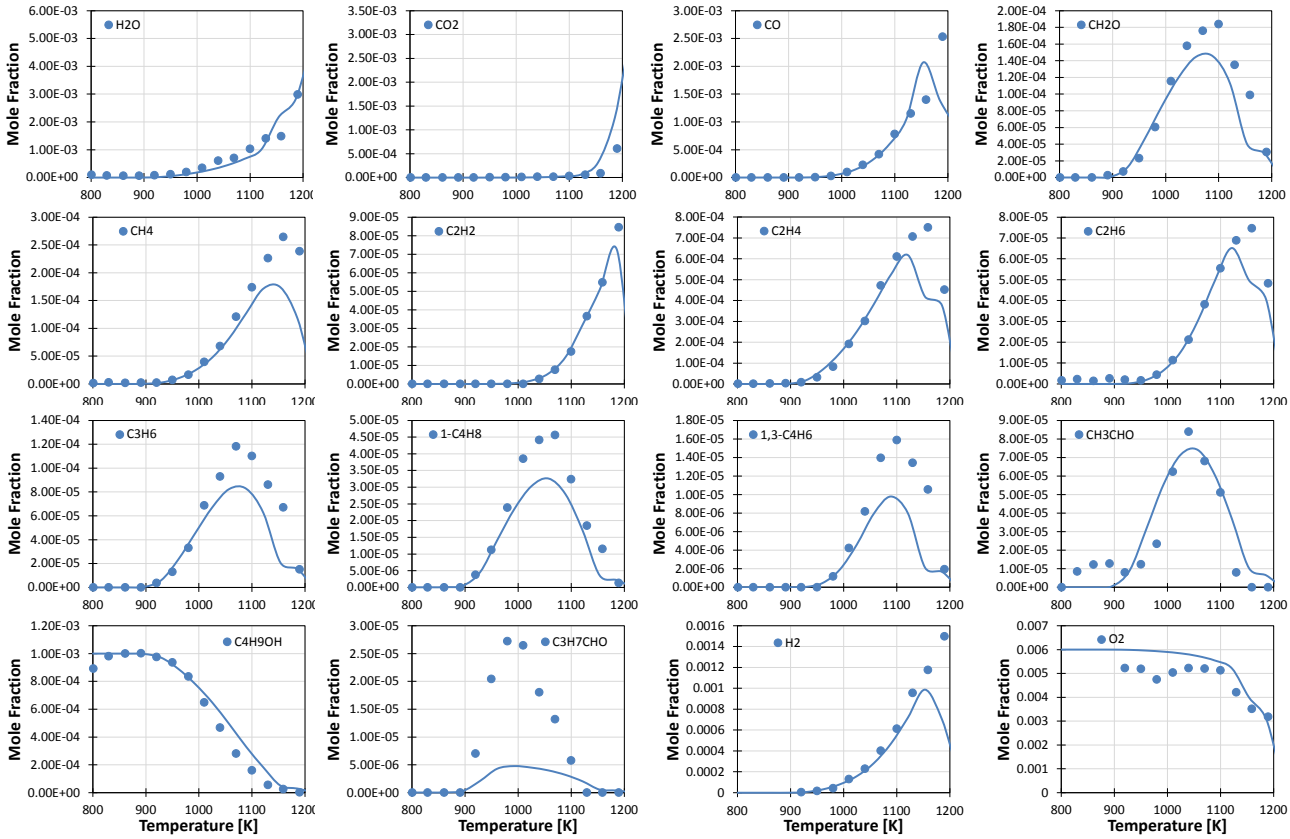

Figure 16: n-butanol (0.1% mol)/O_2/N_2 oxidation in JSR at φ = 1.0, p = 1 bar and τ = 0.07 s. Comparison between experimental (symbols) [7] and predicted (lines) mole fraction profiles of intermediate and product species.

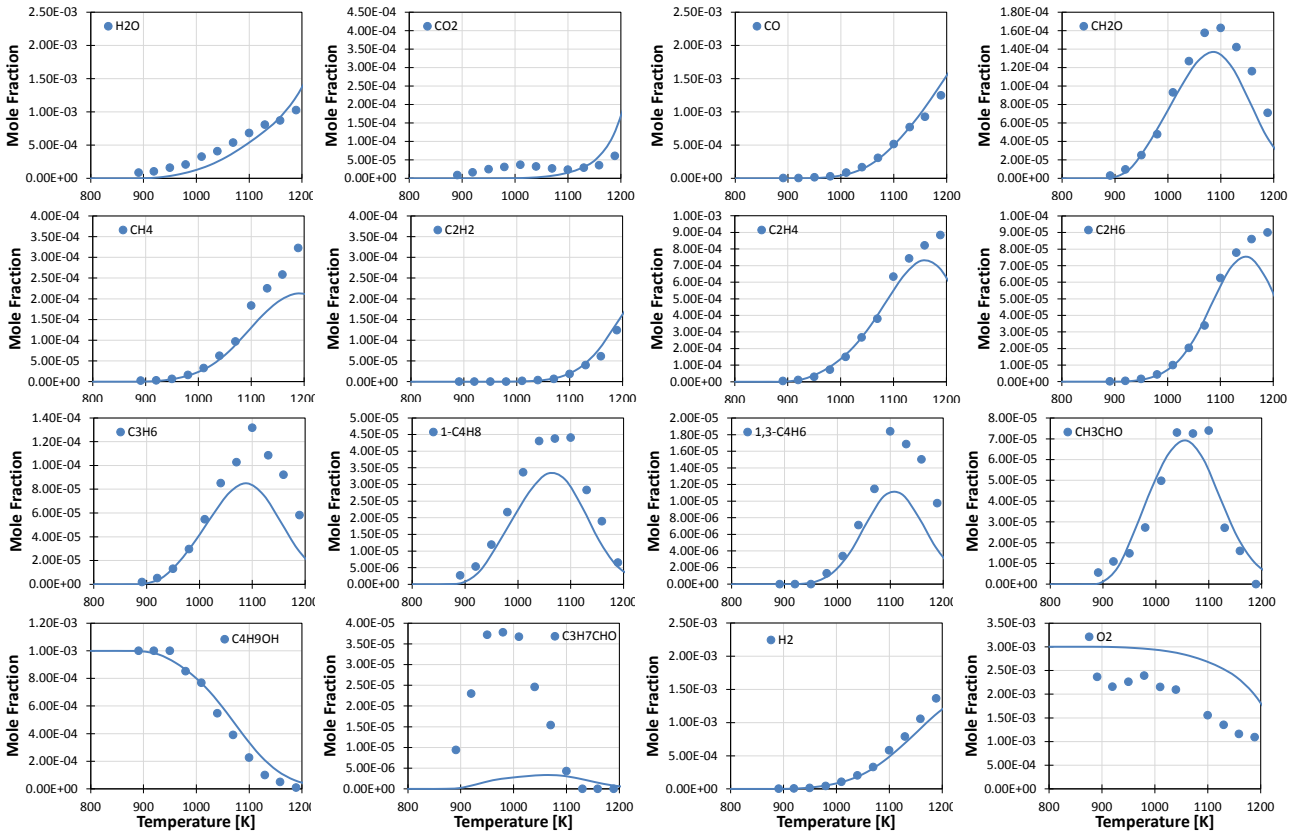

Figure S17: n-butanol (0.1% mol)/O_2/N_2 oxidation in JSR at φ = 2.0, p = 1 bar and τ = 0.07 s. Comparison between experimental (symbols) [7] and predicted (lines) mole fraction profiles of intermediate and product species.

Figure S18 compares the model presented in this work with that of Sarathy et al. [4] for the oxidation of a stoichiometric *n*-pentanol (0.1 % mol)/O_2/N_2 mixture at p=10 bar and τ=0.7 s.

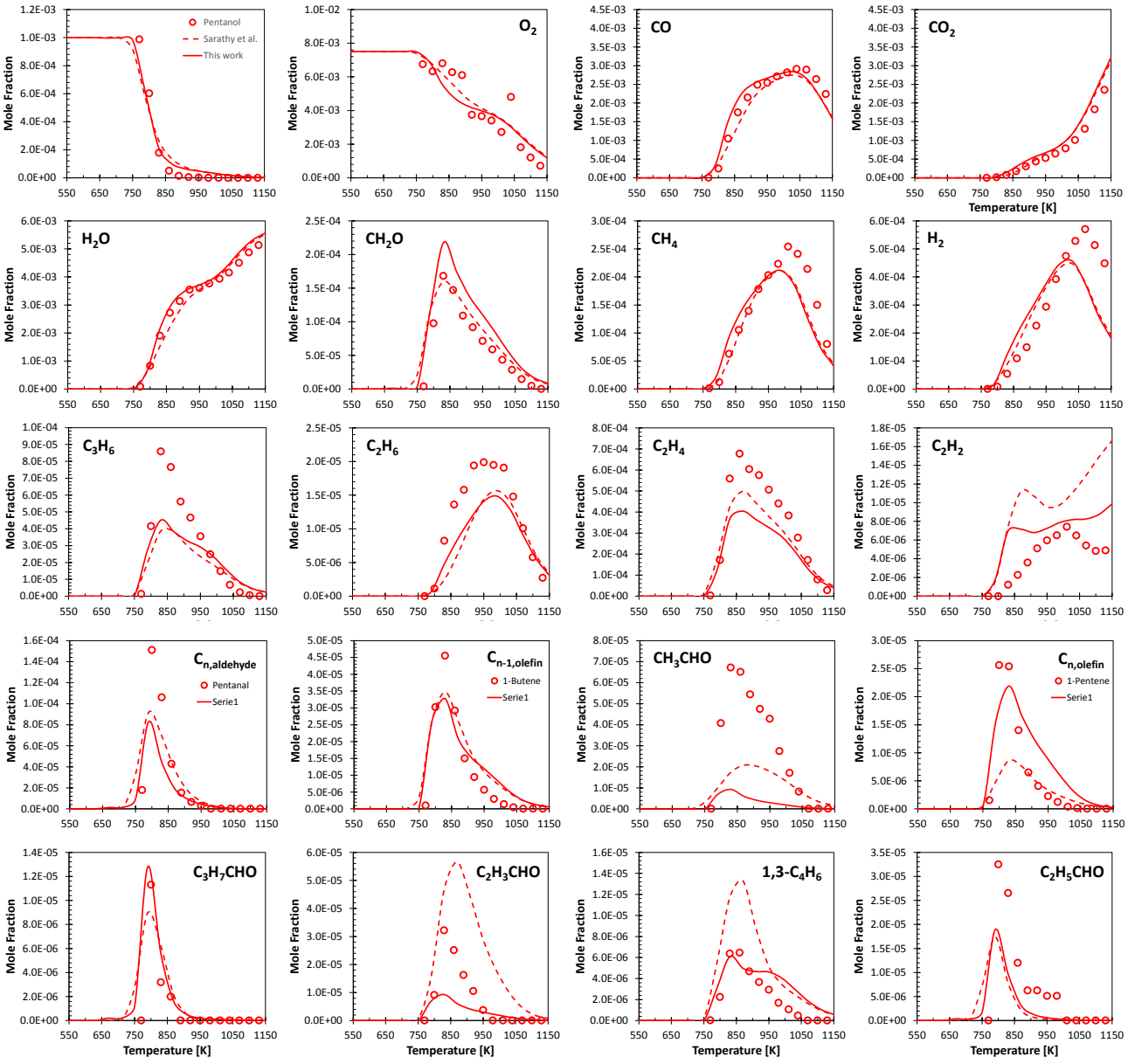

Figure S18: Experimental (symbols) [9] and simulated (lines) mole fraction profiles of n-pentanol oxidation at p = 10 bar and φ=1.0. Dashed lines: Sarathy et al. [4], solid lines: this work.

Ignition delay time [10-20]

This section compares experimental ignition delay times from the literature with model predictions for *n*-propanol, *n*-butanol, *n*-pentanol and *n*-hexanol.

n-propanol

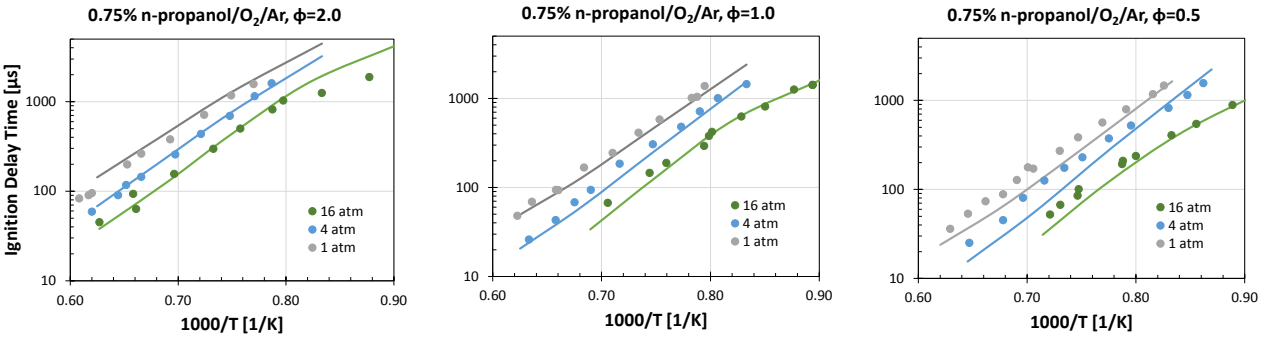

Figure S19: Experimental (symbols) [11] ignition delay times and results from model simulations (lines) for 0.75% mol n-propanol/O_2/Ar mixtures at different pressures and equivalence ratios φ.

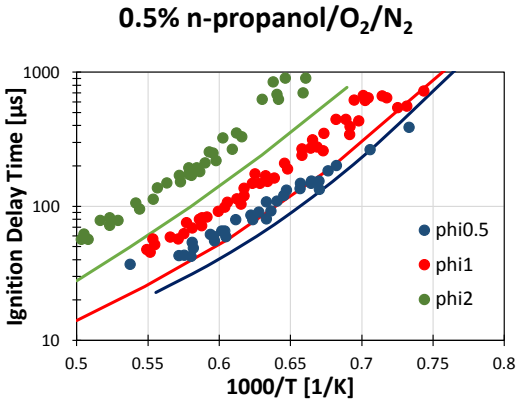

Figure S20: Experimental (symbols) [10] ignition delay times and results from model simulations (lines) for 0.5% mol n-propanol/O_2/Ar mixtures at atmospheric pressure and φ=0.5, 1.0, 2.0.

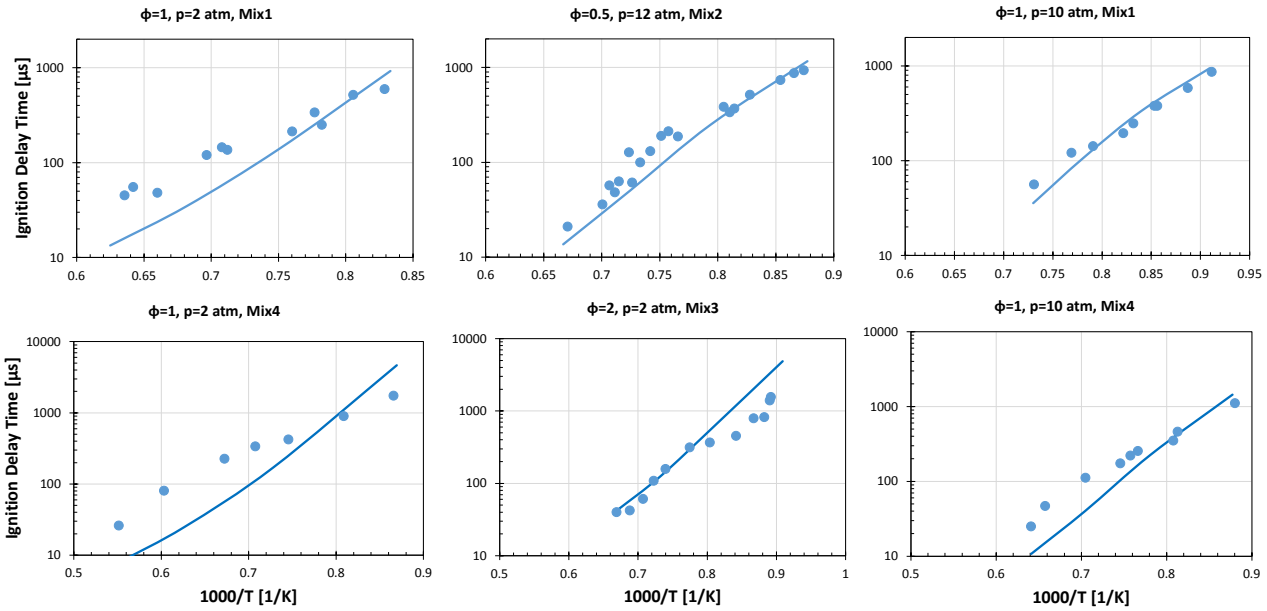

Figure S21: Experimental (symbols) [12] ignition delay times and results from model simulations (lines) for n-propanol/O_2/Ar mixtures at p=1-12 atm, and φ=0.5, 1.0, 2.0. The reader is referred to the study of Noorani et al. for mixture compositions.

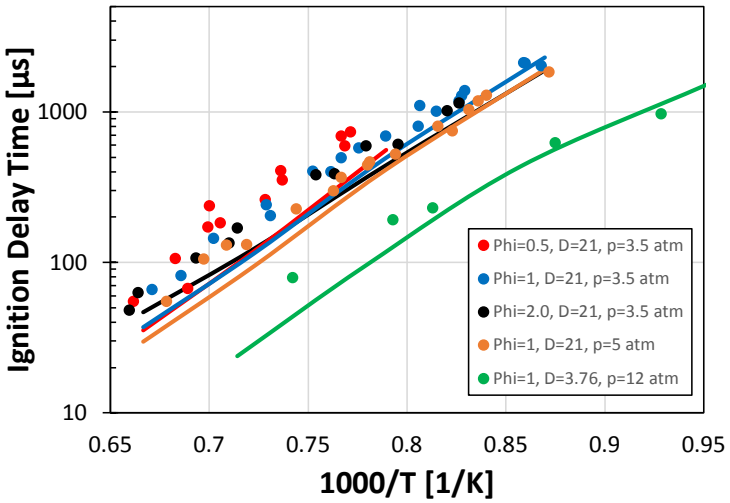

Figure S22: Experimental (symbols) [13] ignition delay times and results from model simulations (lines) for n-propanol/O_2/Ar mixtures at p=3.5-12 atm, φ=0.5, 1.0, 2.0 and varying dilution levels (D). The reader is referred to the study of Jouzdani et al. for mixture compositions and definition of D.

n-butanol

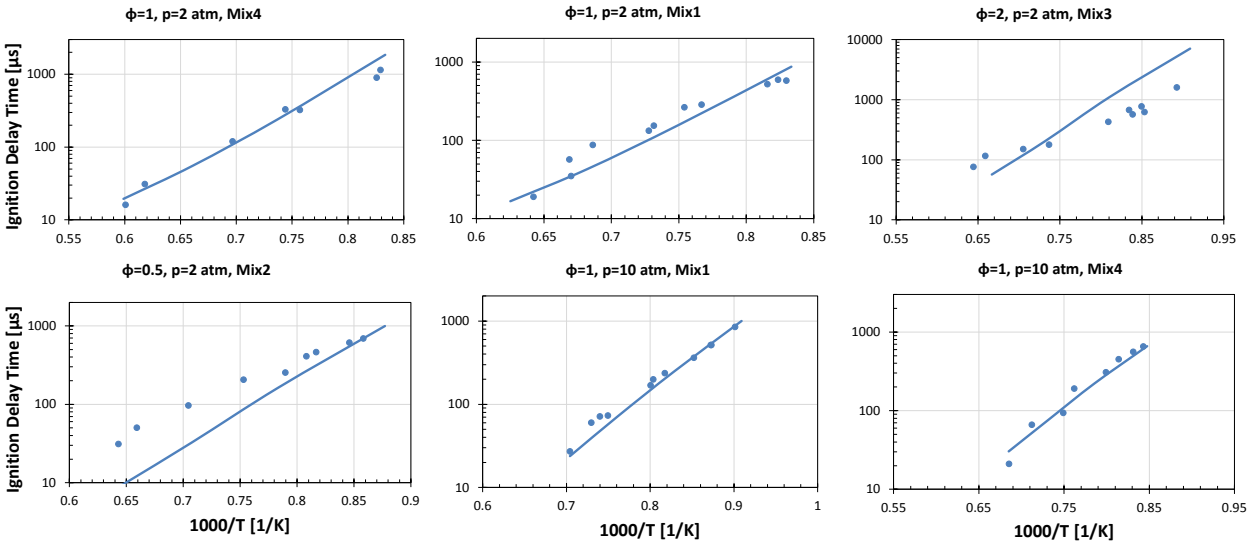

Figure S23: Experimental (symbols) [12] ignition delay times and results from model simulations (lines) for n-butanol/O_2/Ar mixtures at p=1-12 atm, and φ=0.5, 1.0, 2.0. The reader is referred to the study of Noorani et al. for mixture compositions.

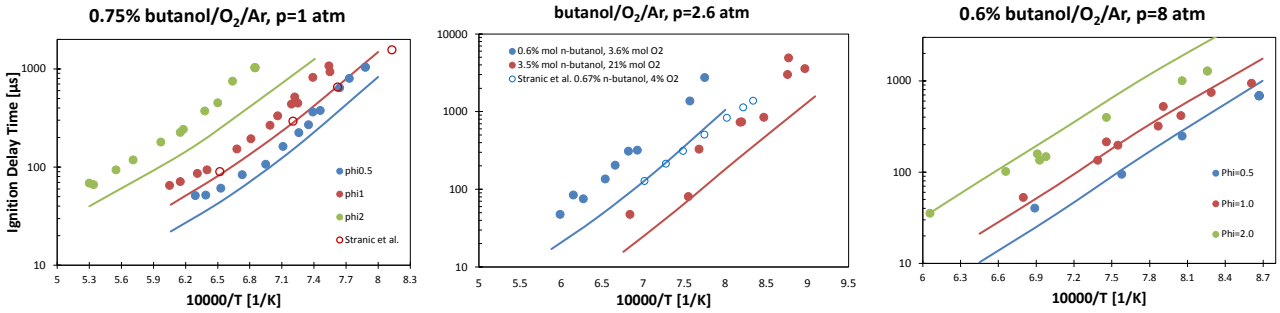

Figure S24: Experimental (symbols) [14] ignition delay times and results from model simulations (lines) for n-butanol/O_2/Ar mixtures at p=1-8 atm, and φ=0.5, 1.0, 2.0 and varying fuel concentration (0.6-3.5% mol). The reader is referred to the study of Black et al. for mixture compositions.

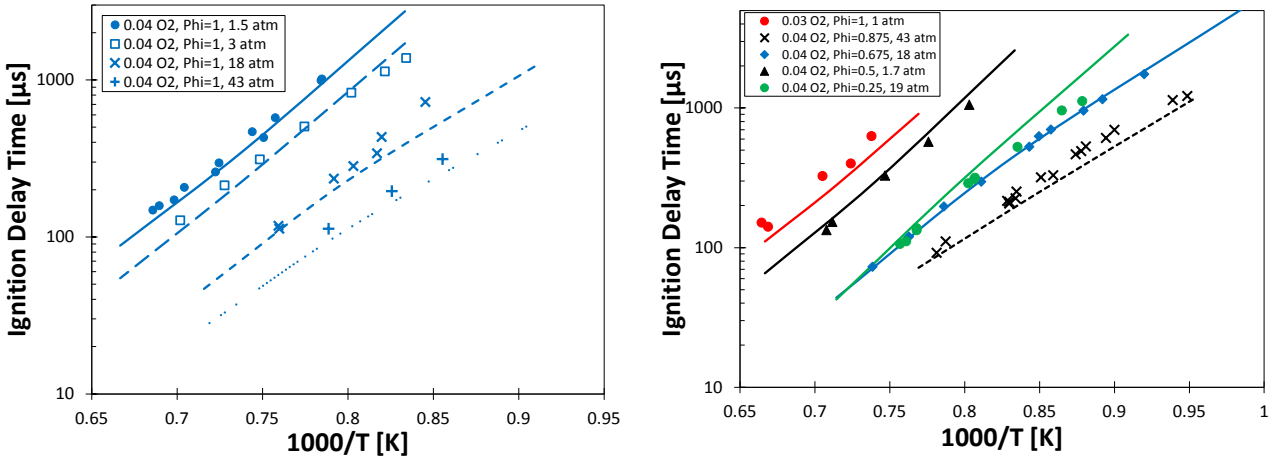

Figure S25: Experimental (symbols) [15] ignition delay times and results from model simulations (lines) for n-butanol/O_2/Ar mixtures at p=1-43 atm, and φ=0.5, 1.0, 2.0 and varying fuel concentration. The reader is referred to the study of Stranic et al. for mixture compositions.

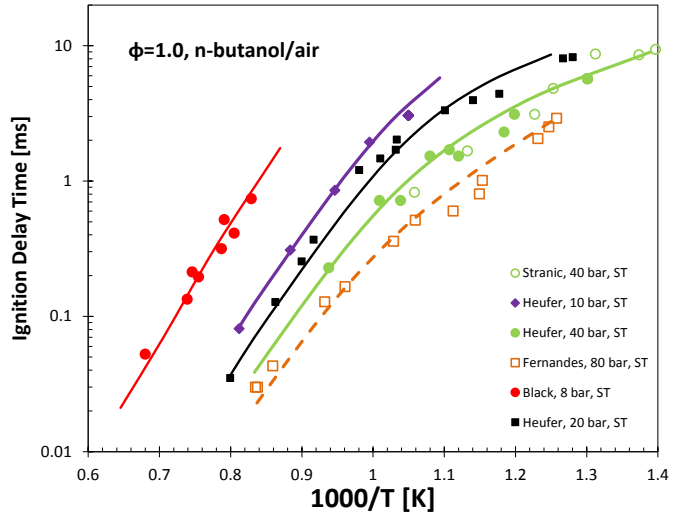

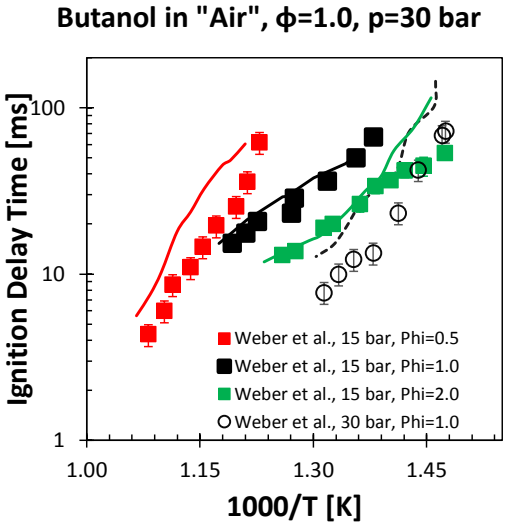

Figure S26: Experimental (symbols) [17, 20, 21] ignition delay times and results from model simulations (lines) for n-butanol/air mixtures at p=8-80 bar, and φ=1.0.

n-pentanol

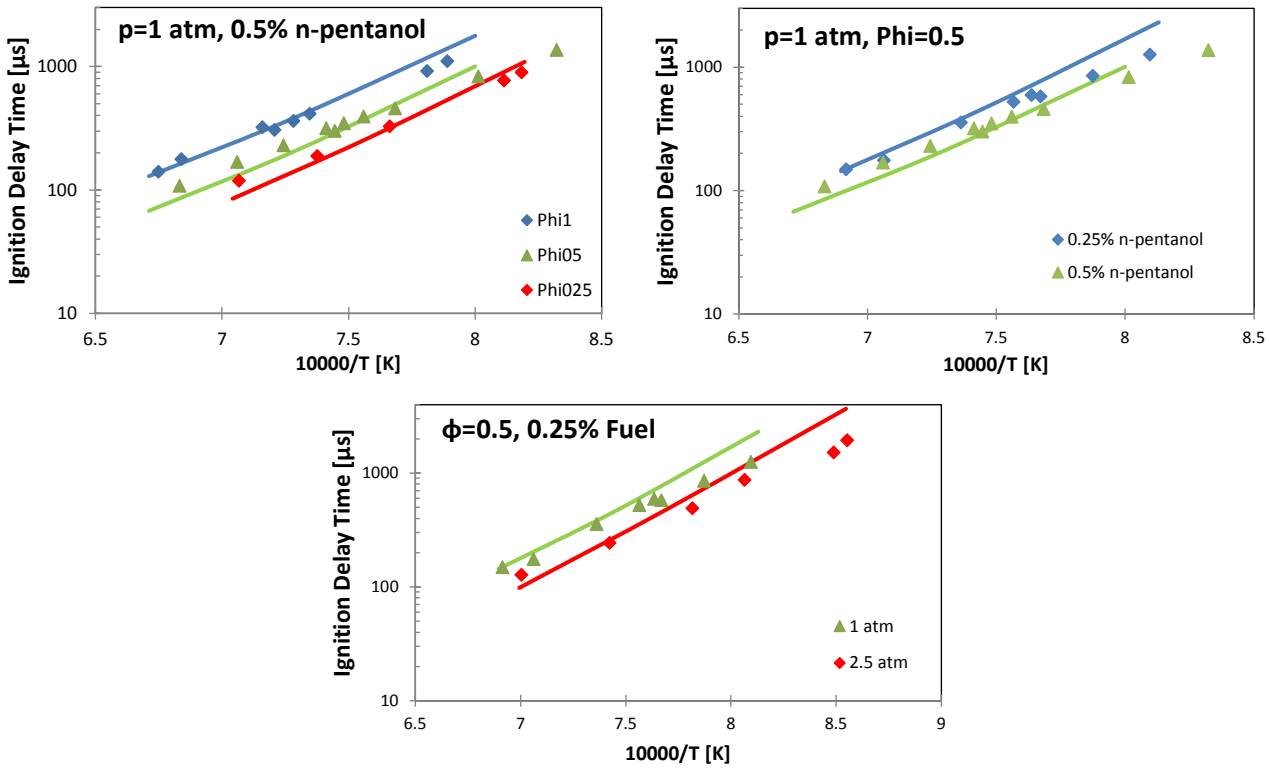

Figure S27: Experimental (symbols) [19] ignition delay times and results from model simulations (lines) for n-pentanol/O_2/Ar mixtures at p=1 atm, and φ=0.5, 1.0, 2.0 and varying fuel concentration (0.25-0.5% mol). The reader is referred to the study of Tang et al. for mixture compositions.

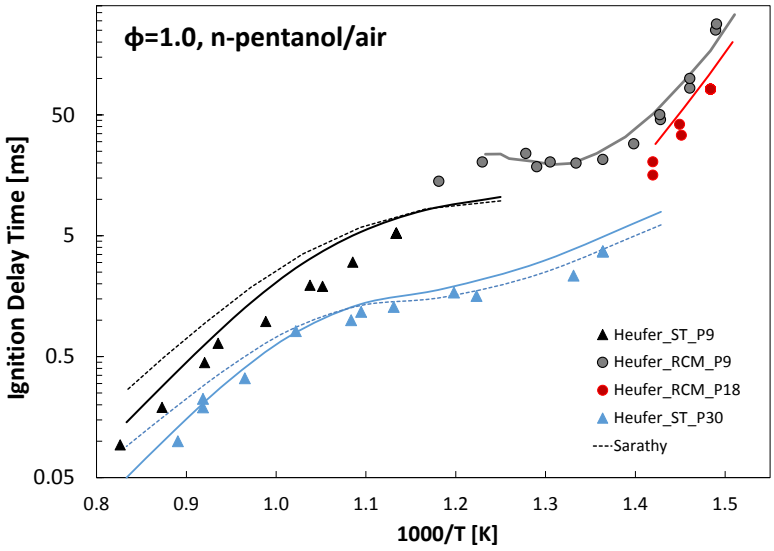

Figure S28: Experimental (symbols) [16, 18] ignition delay times and results from model simulations (lines) for n-pentanol/air mixtures at p=9-30 bar, and φ=1.0.

n-hexanol

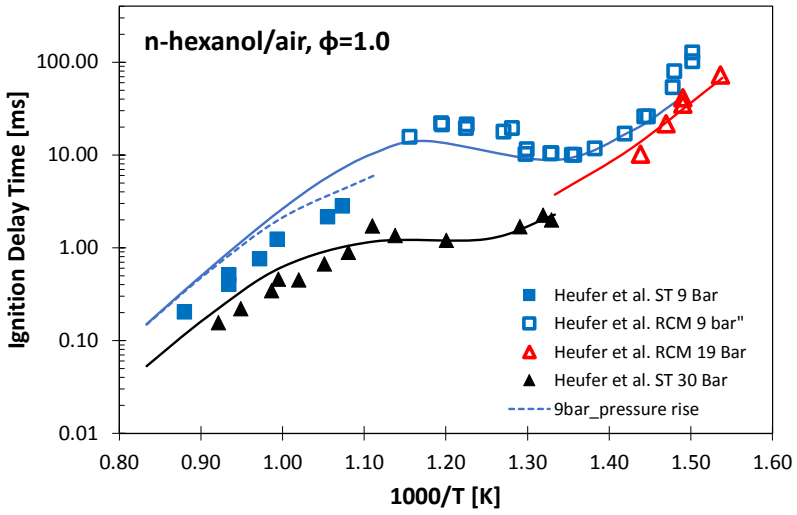

Figure S29: Experimental (symbols) [16] ignition delay times and results from model simulations (lines) for n-hexanol/air mixtures at p=9-30 bar, and φ=1.0.

Laminar Flame Speed

This section compares experimental laminar flame speeds from the literature with model predictions for *n*-propanol, *n*-butanol, *n*-pentanol and *n*-hexanol.

n-propanol [1, 22-25]

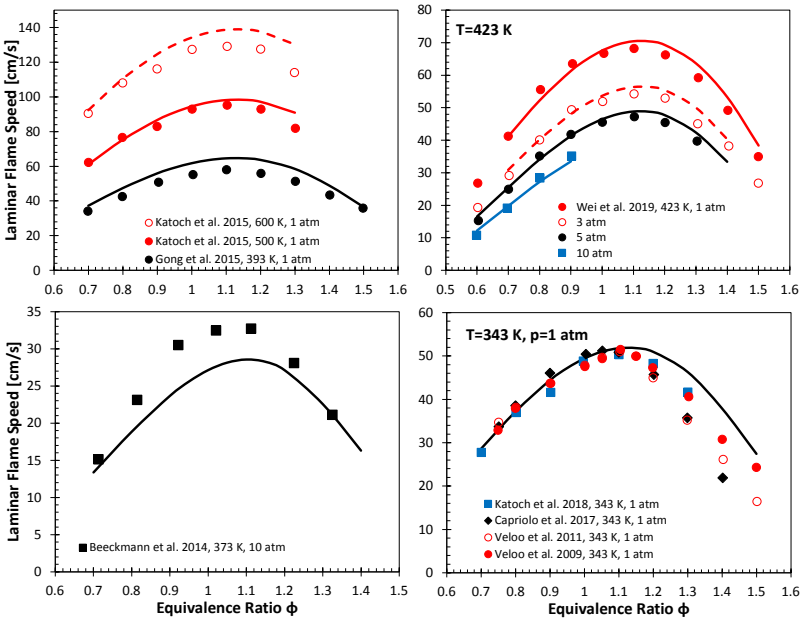

Figure S30: Experimental (symbols) laminar flame speed of n-propanol/air mixtures at T=343-600 K and p=1-10 atm. Lines represent model predictions.

n-butanol [26-31]

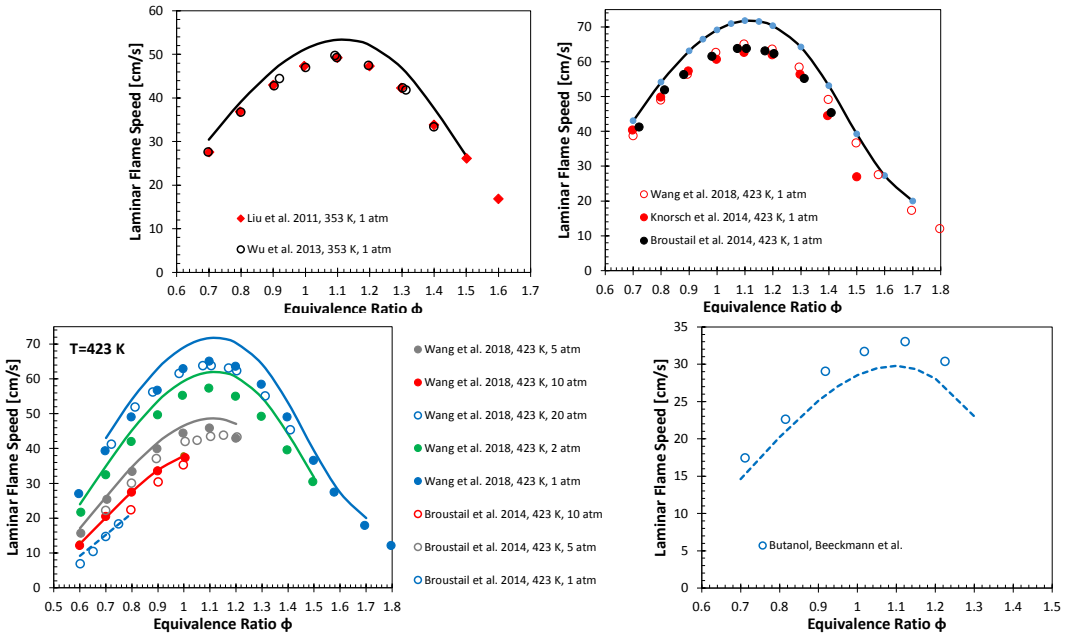

Figure S31: Experimental (symbols) laminar flame speed of n-butanol/air mixtures at T=353-423 K and p=1-20 atm. Lines represent model predictions.

n-pentanol [9, 25, 32-34]

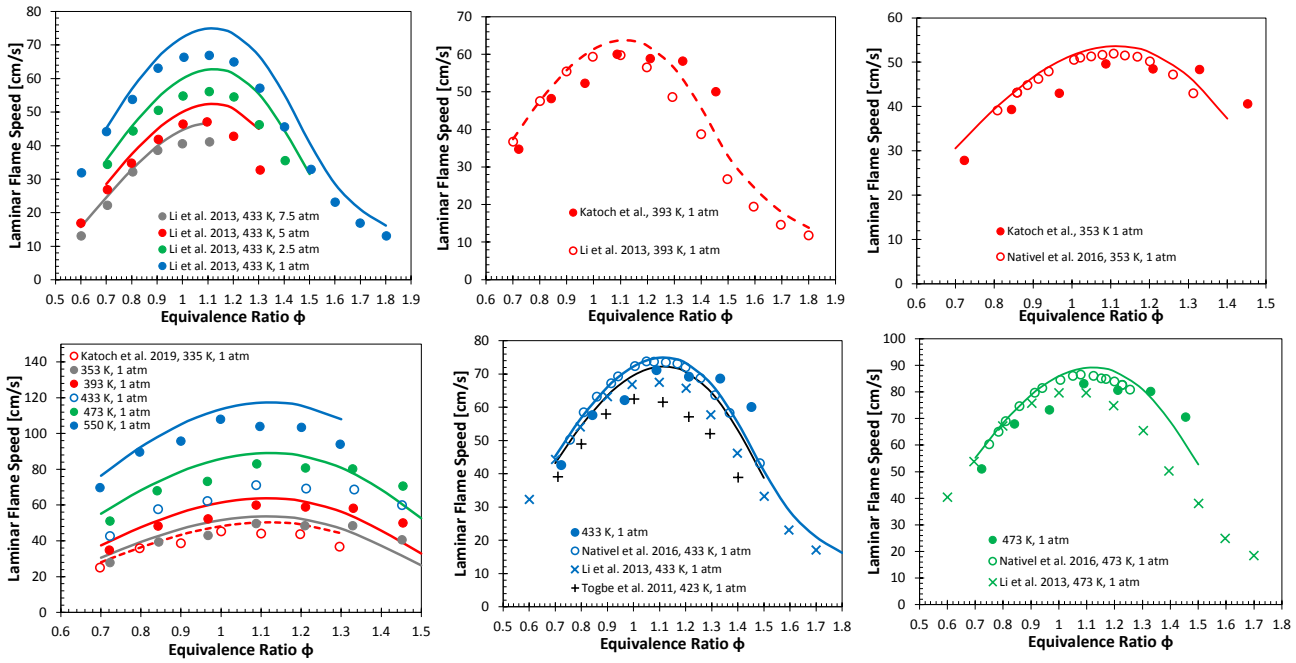

Figure S32: Experimental (symbols) laminar flame speed of n-pentanol/air mixtures at T=353-550 K and p=1-7.5 atm. Lines represent model predictions.

n-hexanol [8, 35]

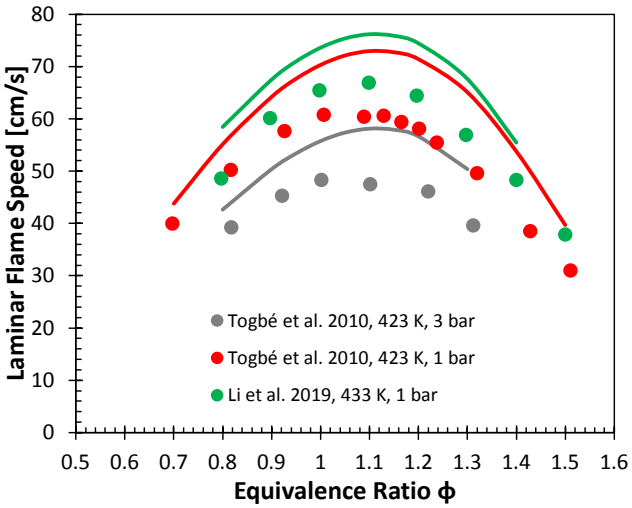

Figure S33: Experimental (symbols) laminar flame speed of n-hexanol/air mixtures at T=423-433 K and p=1 atm. Lines represent model predictions.

4. *n*-Octanol oxidation in a jet-stirred reactor [36]

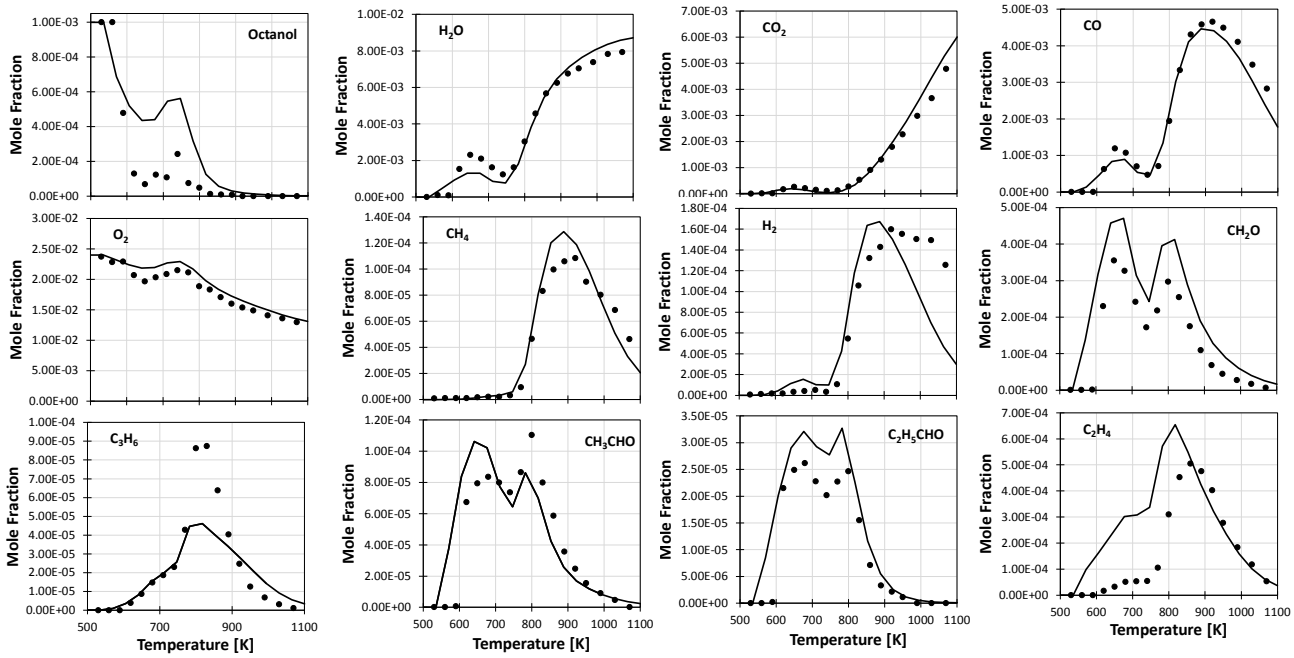

Figure S34: n-Octanol oxidation in a JSR at 10 atm, t = 0.7 s, and φ = 0.5. The inlet fuel mole fraction is 1000 ppm. Symbols denote the experimental data [36] and solid lines show numerical results.

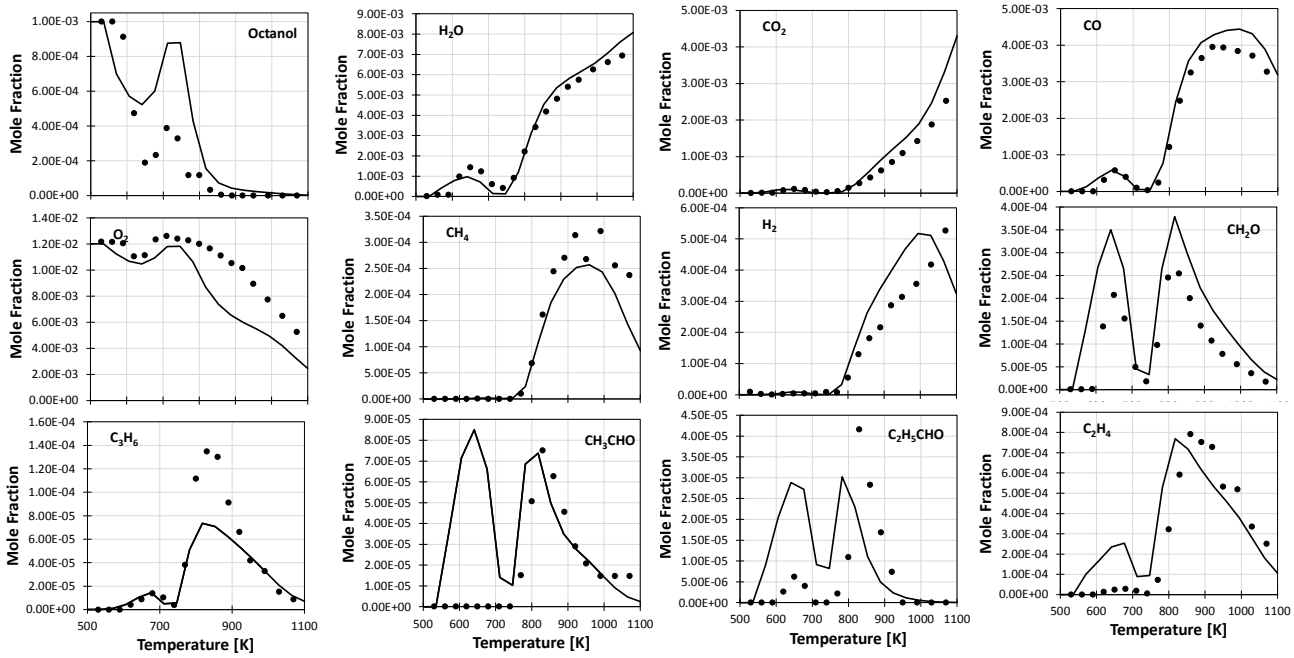

Figure S35: n-Octanol oxidation in a JSR at 10 atm, t = 0.7 s, and φ = 1.0. The inlet fuel mole fraction is 1000 ppm. Symbols denote the experimental data [36] and solid lines show numerical results.

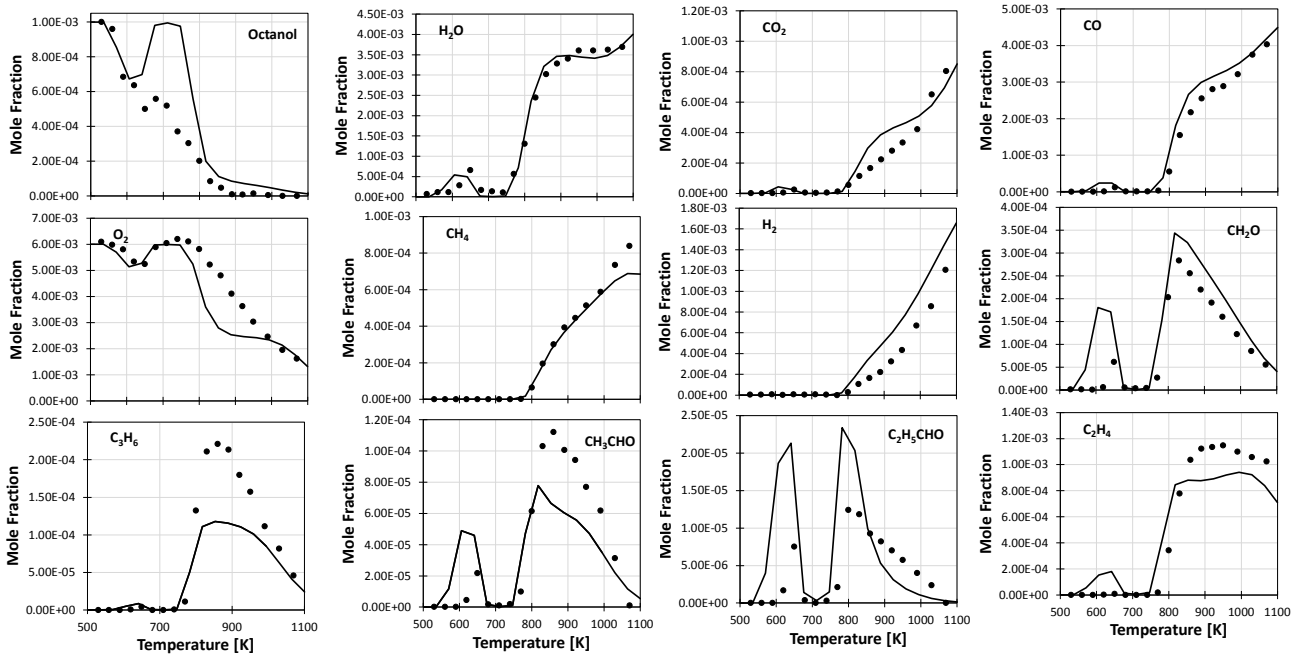

Figure S36: n-Octanol oxidation in a JSR at 10 atm, t = 0.7 s, and φ = 2.0. The inlet fuel mole fraction is 1000 ppm. Symbols denote the experimental data [36] and solid lines show numerical results.

---

5. Additional analyses

Figure S37 shows a sensitivity analysis of ignition delay times to rate constants for *n*-propanol at T=1450 K and p=2 atm.

The impact of *n*-propanol initiation ($nC_3H_7OH=CH_2OH+C_2H_5$) rate constant on high temperature ignition delay times in low pressure shock tubes and on the pyrolysis experiments are reported in Figure S38.

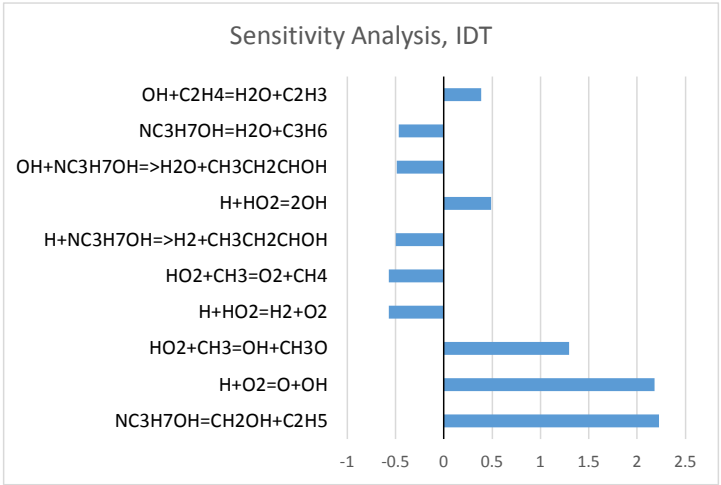

Figure S37: Sensitivity analysis of n-propanol/O_2/Ar ignition delay times to model rate constants at T=1450 K and p=2 atm.

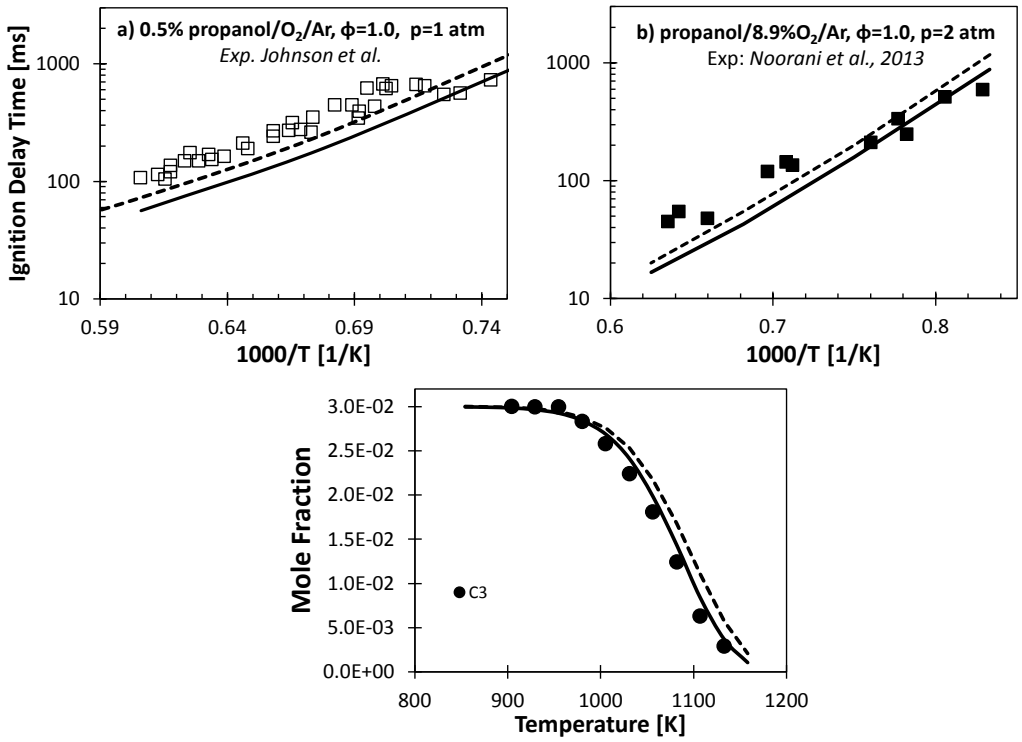

Figure S38: impact of a factor of 2 increase in the initiation rate constant on high temperature ignition delay times of n-propanol/O_2/Ar mixtures (top) and on pyrolysis experiments (bottom).

Figure S39 compares *n*-hexanol and *n*-pentane simulations in an atmospheric pressure JSR at ϕ=0.5.

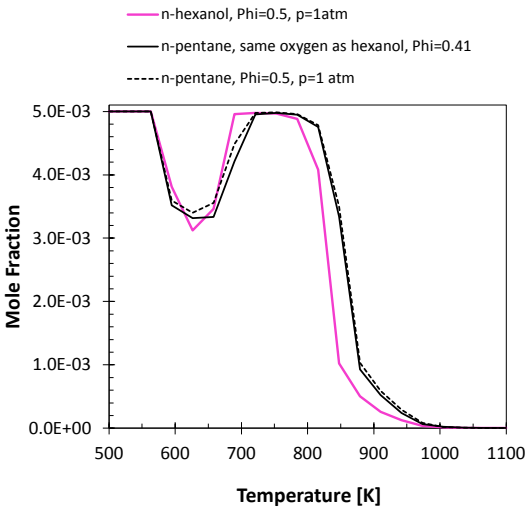

Figure S39: reactivity comparison between n-hexanol and n-pentane for the atmospheric JSR simulations at φ=0.5.

References

[1] W. Li, Y. Zhang, B. Mei, Y. Li, C. Cao, J. Zou, J. Yang, Z. Cheng, Experimental and kinetic modeling study of n-propanol and i-propanol combustion: Flow reactor pyrolysis and laminar flame propagation, Combustion and Flame, 207 (2019) 171-185.

[2] J. Cai, L. Zhang, F. Zhang, Z. Wang, Z. Cheng, W. Yuan, F. Qi, Experimental and kinetic modeling study of n-butanol pyrolysis and combustion, Energy & fuels, 26 (2012) 5550-5568.

[3] G. Wang, W. Yuan, Y. Li, L. Zhao, F. Qi, Experimental and kinetic modeling study of n-pentanol pyrolysis and combustion, Combustion and Flame, 162 (2015) 3277-3287.

[4] S.M. Sarathy, P. Oßwald, N. Hansen, K. Kohse-Höinghaus, Alcohol combustion chemistry, Progress in energy and Combustion Science, 44 (2014) 40-102.

[5] B. Galmiche, C. Togbe, P. Dagaut, F. Halter, F. Foucher, Experimental and detailed kinetic modeling study of the oxidation of 1-propanol in a pressurized jet-stirred reactor (JSR) and a combustion bomb, Energy & fuels, 25 (2011) 2013-2021.

[6] P. Dagaut, S. Sarathy, M. Thomson, A chemical kinetic study of n-butanol oxidation at elevated pressure in a jet stirred reactor, Proceedings of the combustion Institute, 32 (2009) 229-237.

[7] S.M. Sarathy, M.J. Thomson, C. Togbé, P. Dagaut, F. Halter, C. Mounaim-Rousselle, An experimental and kinetic modeling study of n-butanol combustion, Combustion and Flame, 156 (2009) 852-864.

[8] C. Togbe, P. Dagaut, A. Mzé-Ahmed, P. Diévart, F. Halter, F. Foucher, Experimental and detailed kinetic modeling study of 1-hexanol oxidation in a pressurized jet-stirred reactor and a combustion bomb, Energy & fuels, 24 (2010) 5859-5875.

[9] C. Togbé, F. Halter, F. Foucher, C. Mounaïm-Rousselle, P. Dagaut, Experimental and detailed kinetic modeling study of 1-pentanol oxidation in a JSR and combustion in a bomb, Proceedings of the Combustion Institute, 33 (2011) 367-374.

[10] M.V. Johnson, S.S. Goldsborough, Z. Serinyel, P. O'Toole, E. Larkin, G. O'Malley, H.J. Curran, A shock tube study of n- and iso-propanol ignition, Energy & Fuels, 23 (2009) 5886-5898.

[11] X. Man, C. Tang, J. Zhang, Y. Zhang, L. Pan, Z. Huang, C.K. Law, An experimental and kinetic modeling study of n-propanol and i-propanol ignition at high temperatures, Combustion and flame, 161 (2014) 644-656.

[12] K.E. Noorani, B. Akih-Kumgeh, J.M. Bergthorson, Comparative high temperature shock tube ignition of C1− C4 primary alcohols, Energy & fuels, 24 (2010) 5834-5843.

[13] S. Jouzdani, A. Zhou, B. Akih-Kumgeh, Propanol isomers: Investigation of ignition and pyrolysis time scales, Combustion and Flame, 176 (2017) 229-244.

[14] G. Black, H. Curran, S. Pichon, J. Simmie, V. Zhukov, Bio-butanol: Combustion properties and detailed chemical kinetic model, Combustion and Flame, 157 (2010) 363-373.

[15] I. Stranic, D.P. Chase, J.T. Harmon, S. Yang, D.F. Davidson, R.K. Hanson, Shock tube measurements of ignition delay times for the butanol isomers, Combustion and Flame, 159 (2012) 516-527.

[16] K. Heufer, J. Bugler, H. Curran, A comparison of longer alkane and alcohol ignition including new experimental results for n-pentanol and n-hexanol, Proceedings of the Combustion Institute, 34 (2013) 511-518.

[17] K. Heufer, R. Fernandes, H. Olivier, J. Beeckmann, O. Röhl, N. Peters, Shock tube investigations of ignition delays of n-butanol at elevated pressures between 770 and 1250 K, Proceedings of the Combustion Institute, 33 (2011) 359-366.

[18] K.A. Heufer, S.M. Sarathy, H.J. Curran, A.C. Davis, C.K. Westbrook, W.J. Pitz, Detailed kinetic modeling study of n-pentanol oxidation, Energy & Fuels, 26 (2012) 6678-6685.

[19] C. Tang, L. Wei, X. Man, J. Zhang, Z. Huang, C.K. Law, High temperature ignition delay times of C5 primary alcohols, Combustion and Flame, 160 (2013) 520-529.

[20] S. Vranckx, K.A. Heufer, C. Lee, H. Olivier, L. Schill, W. Kopp, K. Leonhard, C. Taatjes, R. Fernandes, Role of peroxy chemistry in the high-pressure ignition of n-butanol–Experiments and detailed kinetic modelling, combustion and flame, 158 (2011) 1444-1455.

[21] B.W. Weber, K. Kumar, Y. Zhang, C.-J. Sung, Autoignition of n-butanol at elevated pressure and low-to-intermediate

temperature, Combustion and flame, 158 (2011) 809-819.
[22] G. Capriolo, A.A. Konnov, Combustion of propanol isomers: Experimental and kinetic modeling study, Combustion and Flame, 218 (2020) 189-204.
[23] J. Gong, S. Zhang, Y. Cheng, Z. Huang, C. Tang, J. Zhang, A comparative study of n-propanol, propanal, acetone, and propane combustion in laminar flames, Proceedings of the Combustion Institute, 35 (2015) 795-801.
[24] P.S. Veloo, F.N. Egolfopoulos, Studies of n-propanol, iso-propanol, and propane flames, Combustion and Flame, 158 (2011) 501-510.
[25] A. Katoch, A. Chauhan, S. Kumar, Laminar burning velocity of n-propanol and air mixtures at elevated mixture temperatures, Energy & fuels, 32 (2018) 6363-6370.
[26] W. Liu, A.P. Kelley, C.K. Law, Non-premixed ignition, laminar flame propagation, and mechanism reduction of n-butanol, iso-butanol, and methyl butanoate, Proceedings of the Combustion Institute, 33 (2011) 995-1002.
[27] G. Wang, Y. Li, W. Yuan, Y. Wang, Z. Zhou, Y. Liu, J. Cai, Investigation on laminar flame propagation of n-butanol/air and n-butanol/O2/He mixtures at pressures up to 20 atm, Combustion and Flame, 191 (2018) 368-380.
[28] F. Wu, C.K. Law, An experimental and mechanistic study on the laminar flame speed, Markstein length and flame chemistry of the butanol isomers, Combustion and Flame, 160 (2013) 2744-2756.
[29] T. Knorsch, A. Zackel, D. Mamaikin, L. Zigan, M. Wensing, Comparison of different gasoline alternative fuels in terms of laminar burning velocity at increased gas temperatures and exhaust gas recirculation rates, Energy & fuels, 28 (2014) 1446-1452.
[30] G. Broustail, P. Seers, F. Halter, G. Moréac, C. Mounaïm-Rousselle, Experimental determination of laminar burning velocity for butanol and ethanol iso-octane blends, Fuel, 90 (2011) 1-6.
[31] J. Beeckmann, L. Cai, H. Pitsch, Experimental investigation of the laminar burning velocities of methanol, ethanol, n-propanol, and n-butanol at high pressure, Fuel, 117 (2014) 340-350.
[32] Q. Li, E. Hu, X. Zhang, Y. Cheng, Z. Huang, Laminar flame speeds and flame instabilities of pentanol isomer–air mixtures at elevated temperatures and pressures, Energy & fuels, 27 (2013) 1141-1150.
[33] Q. Li, C. Tang, Y. Cheng, L. Guan, Z. Huang, Laminar flame speeds and kinetic modeling of n-pentanol and its isomers, Energy & fuels, 29 (2015) 5334-5348.
[34] D. Nativel, M. Pelucchi, A. Frassoldati, A. Comandini, A. Cuoci, E. Ranzi, N. Chaumeix, T. Faravelli, Laminar flame speeds of pentanol isomers: An experimental and modeling study, Combustion and Flame, 166 (2016) 1-18.
[35] Q. Li, H. Liu, Y. Zhang, Z. Yan, F. Deng, Z. Huang, Experimental and kinetic modeling study of laminar flame characteristics of higher mixed alcohols, Fuel Processing Technology, 188 (2019) 30-42.
[36] L. Cai, Y. Uygun, C. Togbé, H. Pitsch, H. Olivier, P. Dagaut, S.M. Sarathy, An experimental and modeling study of n-octanol combustion, Proceedings of the Combustion Institute, 35 (2015) 419-427.